AEDC-TR-69-95



# DETERMINATION OF THE EXCITATION REACTION OF THE OH RADICAL IN $H_2$-$O_2$ COMBUSTION

M. G. Davis and W. K. McGregor, Jr.
ARO, Inc.
and
A. A. Mason
The University of Tennessee Space Institute



October 1969



ROCKET TEST FACILITY
ARNOLD ENGINEERING DEVELOPMENT CENTER
AIR FORCE SYSTEMS COMMAND
ARNOLD AIR FORCE STATION, TENNESSEE

# NOTICES

When U. S. Government drawings specifications, or other data are used for any purpose other than a definitely related Government procurement operation, the Government thereby incurs no responsibility nor any obligation whatsoever, and the fact that the Government may have formulated, furnished, or in any way supplied the said drawings, specifications, or other data, is not to be regarded by implication or otherwise, or in any manner licensing the holder or any other person or corporation, or conveying any rights or permission to manufacture, use, or sell any patented invention that may in any way be related thereto.

Qualified users may obtain copies of this report from the Defense Documentation Center.

References to named commercial products in this report are not to be considered in any sense as an endorsement of the product by the United States Air Force or the Government.

# DETERMINATION OF THE EXCITATION REACTION OF THE OH RADICAL IN $H_2$-$O_2$ COMBUSTION

M. G. Davis and W. K. McGregor, Jr.
ARO, Inc.
and
A. A. Mason*
The University of Tennessee Space Institute



*Associate Professor and Consultant to ARO, Inc.

## FOREWORD

The work reported herein was sponsored by the Air Force Avionics Laboratory (AVRO), Wright-Patterson AFB, Ohio, under Program Element 62403F, Project 4076.

The results of this research test program were obtained by ARO, Inc. (a subsidiary of Sverdrup & Parcel and Associates, Inc.), contract operator of Arnold Engineering Development Center (AEDC), Air Force Systems Command (AFSC), Arnold Air Force Station, Tennessee, under Contract F40600-69-C-0001. The tests were conducted in Propulsion Research Area (R-2E-4) of the Rocket Test Facility (RTF) under ARO Project Numbers RW0634 and RW5910, and the manuscript was submitted for publication on March 28, 1969.

The authors extend acknowledgement to Mr. Burl Neal (AFAL-AVRO) for his support of this program and to the RTF Research Branch personnel of ARO, Inc., for valuable contributions to the research presented to this report, namely, B. L. Seiber for his advice and suggestions throughout the study, R. P. Rhodes, whose advice on the chemical aspects of the problem was invaluable, and C. E. Redman, C. W. Bearden, Jr., and H. R. Simpkins for their assistance in the laboratory.

This technical report has been reviewed and is approved.

Donald W. Ellison
Lt Colonel, USAF
AF Representative, RTF
Directorate of Test

Roy R. Croy, Jr.
Colonel, USAF
Director of Test

## ABSTRACT

The intensity of the OH radiation from the recombination zone of premixed $H_2$-$O_2$ flames is much greater than can be explained by purely thermal considerations. Previous studies have shown that this extra-thermal radiation can be caused by any one of several chemical reactions. The particular reaction responsible for the overpopulation of the excited levels of the OH radical has been elusive. In this study, by means of analytical examination of previous results together with results obtained in new experiments, all except one of these reactions have been eliminated. The only reaction in the group which successfully fits in the scheme of all observed phenomena is

$$H + OH + OH \rightarrow OH^* + H_2O$$

where OH* refers to the excited $A\ ^2\Sigma^+$ state. Measurements were made of the OH concentration, temperature, and radiant intensity from the $A\ ^2\Sigma^+ \rightarrow X\ ^2\Pi_i$ (0, 0) transition at 3064 A in several hydrogen lean $H_2$-$O_2$ flames using spectrometric methods. These flames had different equivalence ratios and were diluted with different quantities of diluent gases. Results from these measurements are used together with the chemical reaction rate equation, corresponding to the chemical reaction above, to calculate a value for the OH excitation rate ($K_{IX}$). The value found is $2.3 \times 10^{-32}$ $cm^6$-molecule$^{-3}$-sec$^{-1}$. The errors involved in the measurements and calculations are discussed.

## CONTENTS



## APPENDIXES

I. ILLUSTRATIONS

Figure

## NOMENCLATURE

| | |
|---|---|
| $A_{J'J''}$ | Probability per second that the atom in state J′ will spontaneously emit a quantum of energy and pass to state J″ |
| a′ | Spectral line broadening parameter |
| $B_{J'J''}$ | Probability per second that the atom in state J′ will emit a quantum of energy and pass to state J″ when simulated by radiation |
| $B_{J''J'}$ | Probability per second that an atom in state J″ will absorb a quantum of energy from the radiation field and pass to state J′ |
| c | Speed of light |
| D | Diluent nonreacting gas |
| E | Energy |
| $\bar{e}$ | Electronic charge |
| $f_M$ | Mole fraction of species M |
| g | Statistical weight |
| h | Planck's weight |
| I | Radiation intensity |
| K | Rotational quantum number |
| k | Boltzmann's constant |
| $k_i$ | Reaction rate for reaction i |
| $k_m$ | Reaction rate for thermal excitation |
| $k_{-m}$ | Quenching collision rate for collisions with species M |
| [M] | Concentration of species M |
| $\bar{M}$ | Molecular weight |
| N, n | Number density |
| $\bar{n}$ | Number of moles |
| P | Absorption coefficient |
| $\bar{P}$ | Pressure |
| p | Resonance yield factor |

| | |
|---|---|
| Q | Radiation density |
| $\overline{R}$ | Universal gas constant |
| T | Temperature |
| v | Vibrational quantum number |
| $\omega$ | Wave number at line center of the designated spectral line |

**SUBSCRIPTS**

| | |
|---|---|
| ch | Chemiluminescence |
| D | Doppler |
| e | Equilibrium concentration |
| J | Energy state |
| N | Natural |
| th | Thermal |
| $\omega$ | Frequency |

# SECTION I
# INTRODUCTION

Spectroscopic studies of the flame emission spectrum of OH in the electronic transition $A\,^2\Sigma^+ \rightarrow X\,^2\Pi_i$ in the wavelength region from 2800 to 3300 Å show that the intensity of radiation from some regions of the flame is much greater than predicted on the basis of thermochemical equilibrium. This extra-thermal radiation can possibly be attributed to (1) concentrations of the OH radical greater than equilibrium concentrations, (2) creation of the OH radical in an excited state through a chemical reaction, (3) excitation of the OH radical during a chemical reaction, or (4) a combination of these.

Studies of extra-thermal radiation in flames have been conducted for many years. The basic interest has been in the understanding and analysis of the processes responsible for this phenomenon. It would be of practical interest (1) to calculate the amount of radiation which would be emitted from a flame if certain variables were known, and the inverse problem (2) to specify certain properties of the flame from observation of flame radiation. The first problem is a very real one and is associated with observation of ultraviolet radiation from rocket exhaust plumes. The second approach might assist in explaining chemical kinetics and other phenomena associated with combustion processes. Both problem areas are of concern in the Rocket Test Facility (RTF).

One of the main difficulties with combustion studies has been in having a combustion flame source that can be analyzed quantitatively. A burner is required that will produce steady flames with a distinct separation between different chemically active regions of the flame. Only during the last 10 years have such burners been available. Consequently, studies of extra-thermal radiation in flames is still in its infancy.

In a rocket test program conducted in Propulsion Research Area (R-2B), radiation measurements showed extra-thermal ultraviolet radiation emitting from the rocket exhaust. The research herein was undertaken in an attempt to explain this extra-thermal radiation and was conducted in Propulsion Research Area (R-2E-4). This research was concerned with the extra-thermal radiation from only the OH radical in hydrogen-oxygen premixed flames. The two basic reasons for this are: (1) OH radiation is present in almost every combustion process, and (2) a storehouse of knowledge is available on the properties of OH. The first task was to reorganize the facts which have been established by experimental work and to summarize them to lay a basis for the study.

An experiment was planned which could be used to quantitatively specify the flame properties. Next, a suitable experimental complex was designed and constructed to carry out the necessary measurements. Finally, a theoretical and experimental program was carried out to isolate the mechanism responsible for extra-thermal OH radiation.

## SECTION II
## HISTORY

### 2.1 FLAME CHARACTERISTICS

A description of flame structure and an explanation of terms used in flame studies are needed to discuss the study of flames. Basically, the flame consists of three zones, or stages, in the combustion process. These are, in the order of their relative positions above the burner, (1) the reaction zone, where the initial chemical reactions and most of the heat release occur, (2) the quasi-equilibrium zone, where recombination reactions continue and shuffling reactions occur with species concentrations decaying toward equilibrium values, and (3) the equilibrium zone, where these equilibrium values have been reached and all chemical reactions are in equilibrium. Although the temperature may be changing as the gases move through the quasi-equilibrium zone, because of heat given or taken up by the recombination reactions, the change is usually very small, and the temperature is essentially constant through this region for most flames. In the equilibrium region, the temperature remains constant for a considerable distance downstream. However, radiation losses and mixing with outside gases slowly reduce the temperature as the gases proceed away from the quasi-equilibrium zone. The geometry and size of these zones change from flame to flame and burner to burner and as functions of pressure.

### 2.2 EVIDENCE OF CHEMILUMINESCENCE IN FLAMES

Evidence of excitation of the OH radical in excess of that expected thermally was first observed by Kondratiev and Ziskin (Ref. 1). They observed that in low-pressure hydrogen flames the vibrational band system of the $A\ ^2\Sigma^+ \rightarrow X\ ^2\Pi_i$ transition of OH showed an abnormal vibrational intensity distribution with bands of $v' = 2$ and 3 being relatively enhanced. They attributed this to the reaction

$$H + H_2 + O_2 \rightarrow H_2O + OH^* \qquad (I)$$

where OH* refers to the excited $A\ ^2\Sigma^+$ state.

Detailed studies of low-pressure acetylene flames were made by Gaydon and Wolfhard (Ref. 2). Their measurements were complicated by the flame structure as shown in Fig. 1 (Appendix I). Radiation received at the spectrograph originated in two or more regions of the flame and made analysis of the data difficult. The most significant results of their work were the excitation temperatures measured by the spectral line reversal of FeI and the rotational temperature from OH emission, especially at low pressures (below 10 mm Hg). These measured temperatures were much higher than the theoretical flame temperature. The results for OH were explained in terms of collisional and radiative deactivation of the electronically excited OH radicals. It was theorized that the OH radicals were formed in the reaction zone as a result of an unknown chemical reaction and that they were formed in the $^2\Sigma^+$ state with a high rotational energy. An average collision diameter was assumed, and it was stated that deactivation by collision appeared to occur on the average about 40 collisions. It was also theorized that deactivation occurred mainly by collisions with $O_2$ molecules.

In subsequent studies, investigators used improved burner designs to give a flat, disc-shaped reaction zone. These flat flame burners produced flames with regions distinctly separated as shown in Fig. 2. This allowed spectroscopic measurements of each region of the flame to be made without interference from the other regions. A sheath of inert gas was flowed around the flames to prevent mixing with the surrounding air so that the spectroscopic measurements would be made through a near isothermal region of the flame.

Gaydon and Wolfhard (Ref. 3) attempted to obtain line reversal temperatures for rotational lines of OH in an acetylene-air flat flame, but the OH concentration was so small at low pressures that absorption lines were hardly detectable. Estimates of the temperature were made for the low rotational quantum number lines of the Q branch of the (0, 0) band and were discovered to be much higher than the adiabatic flame temperature.

## 2.3 THEORIES EXPLAINING EXTRA-THERMAL EXCITATION OF THE OH RADICAL IN FLAMES

### 2.3.1 Preassociation Theory

A phenomenon known as predissociation and preassociation is depicted in Fig. 3. If a diatomic molecule is in electronic state B with a vibrational energy (for the example in Fig. 3, $v' = 3$) large enough to

bring the molecule's total energy up to the energy of the continuum region for a molecule in electronic state A, it may dissociate by undergoing a radiationless transition to electronic state A. In a similar manner, if the two atoms necessary for forming the diatomic molecule in question have a combined energy (for the example in Fig. 3, this energy corresponds to v' = 2) residing in the continuum region of electronic state A, they may directly combine or associate and form a molecule in electronic state B.

In an investigation of OH radiation from the reaction zone of an oxyacetylene flame, Gaydon and Wolfhard (Ref. 4) observed that the rotational lines of the $A\ ^2\Sigma^+ \rightarrow X\ ^2\Pi_i$ (0, 0) transitions with high rotational quantum numbers were weaker than those expected for a Maxwell-Boltzmann distribution. It was thought that this might be a result of a limited amount of energy, less than the energy state corresponding to some rotational quantum number (J) in the $^2\Sigma^+$ state, being available from the chemical processes. This led to the investigation of the rotational intensity distribution of the (1, 0) and (2, 1) bands found at 2811 and 2875 Å, respectively. In investigations of low-pressure oxyacetylene flames, Gaydon and Wolfhard found that there was an abrupt decrease in intensity of the higher rotational levels in the (1, 0) band and that the entire (2, 1) band was weaker than predicted on the basis of thermochemical equilibrium. Detailed examinations showed that this weakening occurred at different energy levels in different vibrational bands. Figure 4 (taken from Ref. 4) illustrates the results found for the (2, 1) and (1, 0) bands.

For the (1, 0) band, the weakening occurred sharply at K' = 18 at an energy of 40,712 $cm^{-1}$. For the (2, 1) band, all rotational levels were affected so that the weakening occurred at or below K' = 0 at 38,221 $cm^{-1}$. For the (0, 0) band, the weakening was less abrupt but seemed to occur for rotational quantum numbers above K' = 25 at 42,630 $cm^{-1}$.

Since the effect did not occur at the same absolute energy in all vibrational states, it was concluded in Ref. 4 that it probably was not due to chemical causes. It could, however, be attributed to predissociation for two reasons. It is normal for predissociation (1) to occur at lower energies in higher vibrational energy states and (2) to show up stronger at low pressures, as was found the case here.

If gases are in complete equilibrium, the OH band intensity distribution and magnitude will be practically unaffected by the existence of predissociation. It was stated that this is due to the fact that, in complete equilibrium where all forms of energy (thermal, radiant, and chemical) are equipartitioned, predissociation must be balanced by preassociation. In this case, it was suggested that the predissociation reaction

$$OH\ (^2\Sigma) \rightarrow O\ (^3P) + H(^2S) \qquad (II)$$

must be balanced at equilibrium by the preassociation reaction

$$O\ (^3P) + H\ (^2S) \rightarrow OH\ (^2\Sigma) \qquad (III)$$

The radicals O and H must be in their ground states ($^3P$ and $^2S$), respectively, since any of their excited states results in an energy greater than the dissociation energy of the upper electronic state of OH, $^2\Sigma$. It is noted that spin is conserved, and reaction (III) is, therefore, a possible reaction as far as spin conservation is concerned.

If a case of nonequilibrium is examined where an excess of free oxygen and hydrogen atoms exists, then the preassociation reaction might dominate, and the vibrational bands for $v' \geq 2$ would be selectively strengthened. For a simple flame of hydrogen burning in air, the three bands (1, 0), (2, 1), and (3, 2) appeared roughly equal in intensity, indicating selective strengthening of levels with $v' = 2$ and 3. Thus, Gaydon and Wolfhard concluded that excess excitation of OH in flames for bands with upper vibrational quantum numbers ($v' \geq 2$), might be explained by the preassociation reaction (Reaction III).

#### 2.3.2 The Three-Body Collision Theory

Independent evidence for the existence of high concentrations of these atoms in $H_2$-rich flames was found by Bulewicz, James, and Sugden (Ref. 5) by examining the reaction

$$Li + H_2O \rightleftharpoons Li\,OH + H \qquad (IV)$$

in flames produced on a flat flame burner. The equilibrium constant for this reaction is known, and the relative H concentration was determined by measuring the red line emission of Li. It increased with H concentration. It was found that the H concentration was very high near the reaction zone and rapidly decayed to a nearly constant value as the flame was axially traversed.

In a later study by Charton and Gaydon (Ref. 6), also using a flat flame burner, measurements were made of the OH radiation of each vibrational band as a function of distance above the burner for premixed $H_2$-$O_2$-$N_2$ flames. This was compared with Li radiation measurements.

The intensities of both rose very rapidly from the base of the flame and then decayed to nearly constant values. Bands of OH arising from higher vibrational levels decayed slower than the (0, 0) band. An example of the (0, 0) band radiation compared with the Li radiation, which is proportional to the H concentration, is shown in Fig. 5 (taken from Ref. 6). The intensity of the (0, 0) band of OH was very strong at the base of the flame and decayed rapidly with distance from the burner face although the temperature changed only slightly. Excess excitation of this band could not be due to preassociation since the term level dissociation energy of OH is 35, 500 $cm^{-1}$ and since the upper vibrational energy for $v' = 0$ is only 32, 682 $cm^{-1}$. It was theorized that the most likely source of excitation was the three-body collision

$$O + H + M \rightarrow OH^* + M \qquad (V)$$

where M is any third body. This reaction is exothermic and would give 4.3 eV, while excitation to the $v' = 0$ level of $OH(^2\Sigma)$ requires only 4.0 eV. Excitation to the $v = 2$ and $v = 3$ levels requires a 4.7 and 5.0 eV, respectively. Therefore, it was suggested that the preassociation theory was correct for these levels since insufficient energy is available from Reaction (V).

### 2.3.3 Recent Three-Body Collision Theory

In studies of rich $H_2$-$O_2$-$N_2$ flames, Kaskan (Ref. 7) reported an equation relating the OH radiation from the first four vibrational levels of the excited electronic state ($^2\Sigma$) to the third power of the concentration of OH in the ground state. The study was conducted with a burner consisting of a cylindrical mixing chamber which was capped with a flat water-cooled porous plug through which the premixed gases were forced. This resulted in flames with low rise velocities.

Bulewicz, James, and Sugden (Ref. 5) found that, in the quasi-equilibrium zone, the species O, H, and OH are in equilibrium with one another although the gas as a whole is still in a state of nonequilibrium. This phenomenon is referred to as partial equilibrium. They explained this to be due to two sets of reactions, one set being very fast, the other relatively slow. The fast reactions reach equilibrium in less than one microsecond after the gas passes through the reaction zone. These reactions are called shuffling reactions since they do not take the gas to true equilibrium. They are given by

$$H_2O + H \underset{K_{-VI}}{\overset{K_{VI}}{\rightleftharpoons}} H_2 + OH \qquad \text{(VI)}$$

$$O + H_2 \underset{K_{-VII}}{\overset{k_{VII}}{\rightleftharpoons}} OH + H \qquad \text{(VII)}$$

$$O_2 + H \underset{K_{-VIII}}{\overset{K_{VIII}}{\rightleftharpoons}} OH + O \qquad \text{(VIII)}$$

The slow reactions serve to bring the gas to complete equilibrium and are called the recombination reactions.

Since Reactions (VI), (VII), and (VIII) are in equilibrium, the concentration of the species involved in each reaction is related by means of an equilibrium constant. The equilibrium constants are functions only of temperature and may be found from the following equations (Ref. 8):

$$\log_{10} K_{VII} = \frac{-3.378473}{T} + 0.8002110 - 0.0557988\,T - 0.0035622\,T^2 \qquad (1)$$

$$\log_{10} K_{VII} = \frac{-3.637429}{T} + 1.3166863 - 0.0691961\,T + 0.0040944\,T^2 \qquad (2)$$

$$\log_{10} K_{VIII} = \frac{-0.399082}{T} + 0.3271011 + 0.0170911\,T - 0.00231636\,T^2 \qquad (3)$$

The equations relating the concentrations of the species are found, using Reactions (VI) through (VIII), to be

$$K_{VI} = \frac{[H_2][OH]}{[H_2O][H]} \qquad (4)$$

$$K_{VII} = \frac{[OH][H]}{[O][H_2]} \qquad (5)$$

$$K_{VIII} = \frac{[OH][O]}{[O_2][H]} \qquad (6)$$

At this point, a distinction needs to be made between rich and lean flames. Rich flames are by definition those in which there are an excess of fuel and a shortage of oxidizer. In this study, then, rich flames are characterized by large concentrations of atomic and molecular hydrogen

and by small concentrations of atomic and molecular oxygen. Similarly, lean flames are characterized by a shortage of fuel and, consequently, have small concentrations of atomic and molecular hydrogen and large concentrations of oxygen. This is summarized by:

[H], $[H_2]$: large in rich flames; small in lean flames

[O], $[O_2]$: small in rich flames; large in lean flames

In a rich $H_2$-$O_2$ flame, the concentrations of $H_2$ and $H_2O$ are always near their equilibrium values outside the reaction zone. This is true because most of the water in flames is formed in the reaction zone and the concentrations of radicals which recombine to form additional water in the recombination zone are very small compared with the concentration of water formed in the reaction zone. The portion of hydrogen found outside the reaction zone in the form of free H is very small. Thus, the majority of hydrogen remains in molecular form ($H_2$) and as a constituent of water in nearly constant concentrations throughout the flame.

By using these facts and Eqs. (4) through (6), the concentrations of O, H, and $O_2$ in a rich flame can be found as functions of OH concentrations by the equations:

$$[H] = \frac{1}{K_{VI}} \frac{[H_2]_e}{[H_2O]_e} [OH] \tag{7}$$

$$[O] = \frac{1}{K_{VI} K_{VII}} \frac{1}{[H_2O]_e} [OH]^2 \tag{8}$$

$$[O_2] = \frac{1}{K_{VII} K_{VIII}} \frac{1}{[H_2]_e} [OH]^2 \tag{9}$$

Kaskan (Ref. 7) measured the OH emission intensity as a function of downstream distance from the (0, 0), (1, 0), (2, 1), and (3, 2) vibrational bands of the $A\ ^2\Sigma^+ \rightarrow X\ ^2\Pi_i$ transition. The radiation was found to be very large near the reaction zone and to decay rapidly downstream. The OH concentration was also measured at the same points by the spectral line absorption method. When the intensity of each band was plotted as a function of OH concentration on log-log paper, the result was a straight line with a slope of 3 as shown in Fig. 6 (taken from Ref. 7). This shows that the measured OH radiation was proportional to $[OH]^3$. Kaskan also attempted measurements in $H_2$-lean flames. In these flames, the OH concentrations appeared to be only slowly varying with distance above

the burner face and were very close to equilibrium. The emission intensities also appeared to be only slowly varying except near the reaction zone, suggesting the establishment of equilibrium in a short distance from the reaction zone. Thus, the intensity variation with [OH] could not be accurately obtained.

The possible reactions in rich flames which are energetic enough to excite OH and which have rates proportional to $[OH]^3$ were examined. Kaskan found four such reactions, in addition to the preassociation reaction, which explain the data. These were:

$$H + OH + OH \xrightarrow{K_{IX}} H_2O + OH^* \qquad \text{(IX)}$$

$$O + H + M \xrightarrow{K_X} M + OH^* \qquad \text{(X)}$$

$$O + H_2 + OH \xrightarrow{K_{XI}} H_2O + OH^* \qquad \text{(XI)}$$

$$H + O_2 + H_2 \xrightarrow{K_{XII}} H_2O + OH^* \qquad \text{(XII)}$$

By using Eqs. (7) through (9), it is verified that each of these does have a rate proportional to $OH^3$. Each reaction showed regularities with the data, but one was indistinguishable from the other as far as proving which one led to OH chemiluminescence. The excess energy ($\Delta E$) available from each reaction for each of the first four vibrational energy levels for $OH(^2\Sigma^+)$ is shown in Table I, Appendix II (taken from Ref. 7). The negative signs mean that the reaction cannot go unless much additional energy is supplied from another source, such as energy of translation of the colliding particles. From the data obtained from the rich $H_2$-$O_2$-$N_2$ flame and the assumption that the preassociation reaction, Reaction (III), is the cause for excess excitation of the $v' = 2$ and $v' = 3$ vibrational levels of $^2\Sigma$, it is seen that any of the Reactions (IX) through (XII) might be the reaction for causing excess excitation to the $v' = 0$ and $v' = 1$ levels.

## SECTION III
## THEORY

### 3.1 BASIS OF THEORY

Examination of the OH radiation as a function of OH concentration in lean $H_2$-$O_2$ flames may allow the identification of the reaction responsible for the excess excitation of OH. Kaskan (Ref. 9), using a low rise velocity, porous, flat flame burner, found that, in $H_2$-lean flames, the OH

concentration never exceeded the equilibrium value by more than an order of magnitude and then only near the reaction zone where it decreased rapidly to its equilibrium value.

This is in contrast to $H_2$-rich flames where Kaskan (Ref. 10) found the OH concentration to be several orders of magnitude greater than its equilibrium value and persisted for a relatively greater distance downstream. This greater spatial extent of excess OH allowed the measurement of OH radiation as a function of OH concentration in the $H_2$-rich flame. The low rise velocity of the porous burner coupled with the relatively larger OH concentration gradient in lean flames prevented Kaskan from making similar measurements in the $H_2$-lean flame. He also found that $H_2$-lean flames were difficult to stabilize on porous burners.

In the quasi-equilibrium zone of a rich flame, it was found that Reactions (VI) through (VIII) were in equilibrium. Until recently, experimental evidence demonstrating these reactions to be in equilibrium throughout the flame zone for lean flames has not been available. Studies of recombination reactions in highly diluted, lean $H_2$-$O_2$-A mixtures composed of 97-percent argon were made in shock tubes by Getzinger and Schott (Ref. 11). It was found that Reactions (VI) through (VIII) were also in equilibrium in lean flames.

If it is assumed that the partial equilibrium conditions are true for lean nondiluted, or slightly diluted $H_2$-$O_2$ flames, then the chemical reaction can be isolated, which accounts for the chemiluminescence of OH. If a burner could be constructed that would provide a steady, lean flame with high rise velocity such that spatial resolution is increased, then experimental data could be obtained to test the validity of the partial equilibrium assumption. This is the approach undertaken in this work.

### 3.2 THEORY OF OH CHEMILUMINESCENCE IN LEAN $H_2$-$O_2$ FLAMES

In lean $H_2$-$O_2$ flames, the purpose of assuming partial equilibrium is similar to that found in rich flames. It allows the expression of the concentrations of H, $H_2$, and O in terms of the concentration of OH. Since the concentrations of $H_2O$ and $O_2$ will be essentially at their equilibrium values throughout the flame and can be considered constant, then Eqs. (4) through (6) may be used to find the concentrations to be

$$[H] = K_H \frac{1}{[H_2O]_e [O_2]_e} [OH]^3, \quad K_H = \frac{1}{K_{VI} K_{VII} K_{VIII}} \tag{10}$$

$$[H_2] = K_{H_2} \frac{1}{[O_2]_e} [OH]^2 , K_{H_2} = \frac{1}{K_{VII} K_{VIII}} \quad (11)$$

$$[O] = K_O \frac{1}{[H_2O]_e} [OH]^2 , K_O = \frac{1}{K_{VI} K_{VII}} \quad (12)$$

By examining the Reactions (IX) through (XII) as the possible chemiluminescent reactions and using Eqs. (10) through (12), it can be shown that each reaction will yield a chemiluminescent intensity proportional to $[OH]^5$ in a lean flame. As an example, consider Reaction (IX). The kinetic equation for this reaction is

$$\frac{d[OH]^*}{dt} = K_{IX} [H] [OH]^2 \quad (13)$$

If the value for [H] in Eq. (10) is substituted into Eq. (13), then it is found that

$$\frac{d [OH]^*}{dt} = K_{IX} K_{II} \frac{1}{[H_2O]_e [O_2]_e} [OH]^5 \quad (14)$$

Each of the Reactions (IX) through (XII) has the form of

$$U + V + W \xrightarrow{k_i} [OH]^* + X \quad (XIII)$$

This general reaction can be used to develop a theory to explain the extra-thermal excitation of the OH radical. Experimental results may then be examined in the light of the theory and, combined with Kaskan's results (Ref. 7) of the $H_2$-rich flames, used to isolate the reaction responsible for the excitation.

Processes which must be considered in addition to the chemiluminescent reaction are thermal excitation,

$$OH - M \xrightarrow{k_m} OH^* + M \quad (XIV)$$

and quenching

$$OH^* + M \xrightarrow{k_{-m}} OH + M^* \quad (XV)$$

At a particular station in the flame, the differential equation for the rate of change of excited OH may be written as

$$\frac{d[OH]^*}{dt} = k_i [U][V][W] + \sum_m k_m [M][OH] - \sum_m k_{-m} [M][OH]^* - A[OH]^* \qquad (15)$$

The first term on the right side of the equation represents the production of excited OH by one of the chemiluminescent Reactions (IX) through (XII). The second term represents the production of excited OH by thermal excitation. The third term represents the depletion of OH by quenching. The last term represents the depletion of OH by radiative transition. At a particular station in the flame, the number of OH radicals being excited is equal to the number being de-excited, and a steady-state solution is possible. Therefore,

$$\frac{d[OH]^*}{dt} = 0 \qquad (16)$$

and Eq. (15) can be solved for (OH)*. This results in

$$[OH]^* = \frac{1}{A + \sum_m k_{-m} [M]} \left[ k_i [U][V][W] - \sum_m k_m [M][OH] \right] \qquad (17)$$

The number of quanta emitted per second per unit volume (Q) is then given by

$$Q = A[OH]^* = \frac{A}{A + \sum_m k_{-m} [M]} \left[ k_i [U][V][W] + \sum_m k_m [M][OH] \right] \qquad (18)$$

The factor $\left(\frac{A}{A + \sum_m k_{-m} [M]}\right)$ is called the resonance yield factor and is commonly designated by p. It is the ratio of excited OH molecules which radiate to the total number which are de-excited by radiation and quenching. For a lean $H_2$-$O_2$-D flame, where D is a diluent gas, the only molecules with high enough concentration to contribute to the quenching would be $H_2O$, $O_2$, and D.

The thermal OH radiation density ($Q_{th}$) from the flame for a particular transition may be written as

$$Q_{th} = \frac{g_e g_v A [OH]}{(p.f.)_e (p.f.)_v} e^{-E/kT} \qquad (19)$$

where, for the transition of interest, $g_e$ and $g_v$ are the electronic and vibrational statistical weights, $(p.f.)_e$ and $(p.f.)_v$ are the electronic and vibrational partition functions, and E is the energy of the upper energy state. If the ground ($^2\Pi$) state concentration of OH and the temperature are known, then $Q_{th}$ can be found from Eq. (19). The last term of Eq. (18) is also the thermal radiation.

The chemiluminescent radiation ($Q_{ch}$) is thus found by subtracting Eq. (19) from Eq. (18). The result is

$$Q_{ch} = Q - Q_{th} = \frac{A}{A + \sum_m k_{-m}[M]} k_i [U][V][W] \qquad (20)$$

The unknowns in this equation are the resonance yield factor, knowledge of the reaction involved, and its excitation reaction rate ($k_i$).

## SECTION IV
## EXPERIMENTAL THEORY, PROCEDURE, AND APPARATUS

### 4.1 EXPERIMENTAL OBJECTIVES

The first objective was to develop a burner suitable for producing a steady $H_2$-$O_2$ flame with a large rise velocity. The next objective was to measure the parameters which would allow the calculation of the species concentrations in various $H_2$-$O_2$ flames and to measure the total OH radiation resulting from the $A\ ^2\Sigma^+ \longrightarrow X\ ^2\Pi_i$ (0, 0) transition. These measurements were made at various positions along the axis of the flame throughout the quasi-equilibrium zone. As was discussed in Section III, two parameters which would allow calculation of the species concentration in an $H_2$-lean flame are the OH concentration and the temperature. The experimental theory, procedure, and apparatus for finding these parameters are discussed in the following sections.

### 4.2 THEORY FOR MEASUREMENT OF SPECIES CONCENTRATION BY THE SPECTRAL LINE ABSORPTION METHOD

The theory necessary for obtaining an equation for the calculation of species concentration from spectral line absorption measurements is scattered throughout the literature. Therefore, it is summarized here for convenience.

If radiation from a continuum source is directed through a layer of gas, the transmitted beam may show an intensity distribution similar to that in Fig. 7. The gas is said to possess an absorption line at the wave number ($\omega_o$) which is the wave number at the line center. The absorption coefficient ($P_\omega$) of the gas is defined by the equation

$$I_\omega = I_o e^{-P\omega x} \tag{21}$$

where $I_o$ is the intensity of the radiation from the source, $I_\omega$ is the intensity after absorption at wave number ($\omega$), and x is the thickness of the gas layer. From the experimental absorption curve, $P_\omega$ as a function of $\omega$ may be obtained as shown in Fig. 8. The width of this curve at half maximum is called the half width and is designated by $\Delta\omega$. The absorption coefficient of a gas for a particular line is usually given by an expression involving $\omega$, $P_o$, and $\Delta\omega$.

The Einstein transition probabilities are related by the following equations (Ref. 12):

$$A_{J'J''} = 2 h c \omega^3 \frac{g_{J''}}{g_{J'}} \tag{22}$$

$$\frac{B_{J'J''}}{B_{J''J'}} = \frac{g_{J''}}{g_{J'}} \tag{23}$$

$$A_{J'J''} = \frac{1}{\tau} \tag{24}$$

If a beam of light is directed through a layer of gas containing N atoms per unit volume in the ground state and N′ excited atoms per unit volume, then the decrease in the energy of the beam in the spectral range between $\omega$ and $\omega + d\omega$ is given by

$$\begin{aligned} -d[I_\omega \delta\omega] = {} & \delta N_\omega \, d x \, h \omega \, B_{J'J''} \frac{I_\omega}{4\pi} \\ & - \delta N'_\omega \, d x \, h \omega \, B_{J'J''} \frac{I_\omega}{4\pi} \end{aligned} \tag{25}$$

where $\delta N_\omega$ atoms are capable of absorbing in the range between $\omega$ and $\omega + d\omega$ and where $\delta N'_\omega$ atoms are capable of emitting in this range. This may be written to be

$$-\frac{1}{I_\omega} \frac{d I_\omega}{dx} \delta\omega = \frac{h\omega}{4\pi} (B_{J''J'} \delta N_\omega - B_{J'J''} \delta N'_\omega) \tag{26}$$

Differentiating Eq. (21) and dividing by $I_\omega$ results in

$$-\frac{1}{I_\omega}\frac{dI_\omega}{dx} = P_\omega \tag{27}$$

Using this result in Eq. (26) yields

$$P_\omega \delta_\omega = \frac{h\omega}{4\pi}\left(B_{J''J'}\,\delta N_\omega - B_{J'J''}\delta N'_\omega\right) \tag{28}$$

Integration over the entire absorption line, assuming that $\delta\omega \ll \omega$, gives

$$\int_{\delta\omega} P_\omega\, d\omega = \frac{h\omega_o}{4\pi}\left(B_{J''J'}N_{J''} - B_{J'J''}N_{J'}\right) \tag{29}$$

By using Eqs. (22) and (23) which relate the transition probabilities, Eq. (29) becomes

$$\int P_\omega\, d\omega = \frac{g_{J'}}{g_{J''}}\frac{N_{J''}}{8\pi c\omega_o^2 \tau}\left[1 - \frac{g_{J''}}{g_{J'}}\frac{N_{J'}}{N_{J''}}\right] \tag{30}$$

In combustion flames, $N_{J'} \ll N_{J''}$, and the second term is negligible compared with the first term so that Eq. (30) may be written as

$$\int P_\omega\, d\omega = \frac{g_{J'}}{g_{J''}}\frac{N_{J''}}{8\pi c\,\omega_o^2 \tau} \tag{31}$$

The f-value of a spectral line is regarded as a measure of the degree to which the ability of an atom to absorb and emit a quantum is like that of a classical oscillating electron. Mitchell and Zemansky (Ref. 12) show that the f-value is related to the lifetime of the state ($\tau$) by the equation

$$\frac{\pi \bar{e}^2}{\bar{m}\,c^2} N_{J''} f_{J'J''} = \frac{g_{J'}}{g_{J''}}\frac{N_{J''}}{8\pi c\,\omega_o^2 \tau} \tag{32}$$

Substituting this result into Eq. (31) yields

$$\int P_\omega\, d\omega = \frac{\pi \bar{e}^2}{\bar{m}\,c^2} N_{J''} f_{J''J'} \tag{33}$$

In the case where Doppler broadening is large and collisional and natural broadening can be neglected, the absorption coefficient is given by the equation (Ref. 12):

$$P_\omega = P_o \exp\left[-\frac{2c\,(\omega - \omega_o)}{\Delta\omega_D}\sqrt{\ell n\, 2}\right]^2 \tag{34}$$

The Doppler width at half intensity is given by

$$\Delta\omega_D = 7.162 \times 10^{-7}\sqrt{\frac{T}{\overline{m}}} \tag{35}$$

where $\overline{M}$ is the molecular weight of the absorbing species. Integrating Eq. (34) over all wave numbers results in

$$\int_o^\infty P_\omega\, d\omega = \frac{1}{2}\sqrt{\frac{\pi}{\ell n\, 2}}\, P_o\, \Delta\omega_D \tag{36}$$

Now equating the right hand sides of Eqs. (33) and (36) results in

$$\frac{\pi\,\overline{e}^2}{\overline{m}\,c^2}\, N_J''\, f_J''_J = \frac{1}{2}\sqrt{\frac{\pi}{\ell n\, 2}}\, P_o\, \Delta\omega_D \tag{37}$$

If, in addition to Doppler broadening, collisional and natural broadening must be considered, then it has been shown by Penner (Ref. 13) that the true integrated line absorption is related to that found by assuming pure Doppler broadening through the broadening parameter a′, where

$$a' = \frac{(\Delta\omega_N + \Delta\omega_c)\,(\ell n 2)^{1/2}}{\Delta\omega_D} \tag{38}$$

with $\Delta\omega_N$ and $\Delta\omega_c$ being the natural and collisional widths at half intensity, respectively. The true integrated absorption coefficient is now written as

$$\int_o^\infty P_\omega\, d\omega = \frac{\sqrt{\frac{\pi}{\ell n\, 2}}\, P_o\, \Delta\omega_D}{2\,[\exp\,(a')^2]\,[\operatorname{erfc} a']} \tag{39}$$

If a knowledge of a′ is available, then it is necessary to measure only the peak absorption coefficient and temperature to calculate the integrated absorption coefficient. Oldenberg and Rieke (Ref. 14) have shown that one method for doing this is to use a source emitting a line much narrower than the absorption line so that, by measuring the peak of the narrow emission line with and without absorption, the peak absorption coefficient ($P_o$) can be calculated. This principle is illustrated in Fig. 9.

For rotational equilibrium, the number density of a molecule in a vibrational-electronic ground state with rotational quantum number J″ is given by

$$N_{J''} = \frac{2J''+1}{(p.f.)_r\,(p.f.)_v}\, N_o \exp\left[-E_{J''}/kT\right] \tag{40}$$

Combining Eqs. (33), (39), and (40), evaluating the constants, and solving for $N_o$ result in

$$N_o = 1.208 \times 10^{12} \frac{(p.f.)_r\,(p.f.)_v\, P_o \Delta\omega_D}{(2J''+1)\, f_{J''J'}\, [\exp(a')^2]\,[\operatorname{erfc} a']} \times \exp\left[E_{J''}/kT\right] \tag{41}$$

If the only unknowns are $P_o$ and T and these quantities are measurable, then the ground state concentrations ($N_o$) can be calculated.

### 4.3 MEASUREMENT OF OH CONCENTRATION AND TEMPERATURE

In order to apply Eq. (41) to the measurement of OH concentration, it is necessary to know the various parameters involved. These parameters are discussed, and the procedures used to make the measurements are described.

Kaskan (Ref. 9) showed that the rotational partition function $[(p.f.)_r]$ could be accurately calculated for OH for T > 1200°K by the approximating expression

$$(p.f.)_r = \frac{kT}{hcB} \tag{42}$$

where B is the rotational constant for the $^2\Pi$ state of OH and is taken as 18.51 $cm^{-1}$. The vibrational partition function was calculated by the use

of the equation

$$(p.f.)_v = \sum_n \exp [En/kT] \tag{43}$$

where $E_n$ is the energy of the vibrational level n of OH as found using the vibrational constants in Herzberg (Ref. 15).

The transition probabilities $A_{J'J''}$ are listed in Dieke and Crosswhite (Ref. 16) and are related to $f_{J''J'}$ by the equation

$$f_{J''J'} = \frac{F\, A_{J'J''}}{2\, J'' + 1} \tag{44}$$

where F is called the transition probability coefficient. The value of F for the $A\ ^2\Sigma^+ \rightarrow X\ ^2\Pi_i$ (0, 0) transition is taken as $3.07 \times 10^{-4}$ sec as found in investigations by Oldenberg and Rieke (Ref. 14). The value of a′ was

$$a' = 450 \frac{P}{T} \frac{\text{atmospheres}}{^\circ K} \tag{45}$$

as found by Kaskan (Ref. 7) by correlations of OH measurements with other observables in flame gases, and he gives the average value obtained in several line width determinations. Figure 10 shows the values of $(p.f.)_r$ and $(p.f.)_v$, and Fig. 11 shows the value of the broadening factor, $[\exp(a')^2]^{-1}\ [\text{erfc } a']^{-1}$, each as a function of temperature.

The rotational line used in this study for the spectral line absorption measurements was the $R_2 3$ line of the $A\ ^2\Sigma^+ \rightarrow X\ ^2\Pi_i$ (0, 0) band found at 3077 Å since it was easily resolved with the spectrometer being used. The value of $A_{J'J''}$ in Eq. (44) for this line as found in Dieke and Crosswhite (Ref. 16) is 8.9. This was later corrected by Learner (Ref. 17) for rotation-vibration interaction to 8.8. The value of $E_{J''}$ for the $R_2^3$ line is given by Dieke and Crosswhite (Ref. 16) to be 289 $cm^{-1}$ above the ground state. The value of $\Delta\omega_D$ as a function of temperature for the $R_2^3$ line shown in Fig. 12. by rewriting Eq. (41) and using the parameters discussed above, the OH concentration can be expressed by

$$[OH] = 4.47 \times 10^{14} \frac{(p.f.)_r\, (p.f.)_v\, P_o\, \Delta\omega_D}{[\exp (a')^2]\ [\text{erfc } a']} \exp [416/T] \tag{46}$$

The peak absorption coefficient per unit path length ($P_o$) was obtained by measuring the intensity of the $R_2^3$ line radiating from a narrow line source both with ($I_{sf}$) and without ($I_s$) the flame in its path. Then $P_o$ was found by the equation

$$P_o = \frac{1}{\ell} \ln \frac{I_s}{I_{sf}} \tag{47}$$

where $\ell$ is the flame thickness.

The only remaining parameter necessary for the calculation of the OH concentration was the temperature. The method used was the infrared emission-absorption technique as described by Brewer and McGregor (Ref. 18). It involved the measurement of the absorptivity [$\alpha_f(\lambda)$] and the radiance [$N_f(\lambda, T)$] at a particular wavelength ($\lambda$). The absorptivity was measured by placing a continuum source behind the burner and measuring the intensity of the radiation at a particular wavelength ($I_s$) and without ($I_{sf}$) a flame in its path. The absorptivity (($\alpha_f(\lambda)$) was found by the equation

$$\alpha_f = \frac{I_s - I_{sf}}{I_s} \tag{48}$$

Modulation of the source and a synchronous rectifier-amplifier was employed to isolate the source from the flame. The radiance of the flame $N_f$ was then measured by blocking the source radiation with a shutter and modulating the flame radiation with a chopper internal to the spectrometer. The radiance of the source was known, and the optics were so arranged that both the source and the flame filled the view angle of the spectrometer. By comparing the recorder deflection obtained with the source and no flame ($d_s$) with the recorder deflection obtained with the flame ($d_f$), the radiance of the flame could be found. The equation was

$$N_f(\lambda, T_f) = \bar{c} \frac{d_f}{d_s} \epsilon_s N_b(\lambda, T_s) \tag{49}$$

where $\epsilon_s$ is the emissivity of the source, $T_f$ is the temperature of the flame, $T_s$ is the temperature of the source, and $\bar{c}$ is a correction due to absorptivity of the cell windows between the source and the flame. The path between the source and the flame was purged with $N_2$ so that moisture present in air would not absorb the source radiation and cause an error in the calculation of $N_f(\lambda, T_f)$. The wavelength used was 2.46 $\mu$, which is at the edge of an $H_2O$ band. This was found to be the optimum wavelength for obtaining accurate values of emission and absorption.

The equation for calculating the temperature, for this particular wavelength, resulting from the method shown by Brewer and McGregor (Ref. 18) is

$$T(°K) = \frac{5845}{\ln\left[1.35 \times 10^{6} \frac{a_f(\lambda)}{N_f(\lambda, T)}\right]} \tag{50}$$

Substituting the value of T, which was calculated using Eq. (50), and the value of $P_o$, which was calculated using Eq. (47), into Eq. (46) results in a value for the OH concentration.

An optics diagram is presented in Fig. 13, showing the arrangement of the spectrometers and optics about the burner as used to make the OH absorption and emission measurements and the infrared emission and absorption measurements.

### 4.4 MEASUREMENT OF OH EMISSION FROM A $^2\Sigma^+ \rightarrow X\ ^2\Pi_i$ (0,0) TRANSITIONS

The method used for measuring the total band emission from the $A\ ^2\Sigma^+ \rightarrow X\ ^2\Pi_i$ (0, 0) transitions of OH was that developed by Kaskan (Ref. 9). He has shown that , by measuring the relative peak height of the (0, 0) band, which occurs at 3090 Å, the relative upper state population as a function of axial distance would be found. He showed such an approximation to be accurate to within 10 percent in the 1200 to 1600°K temperature range, but this has recently been extended and found useful at higher temperatures up to 2600°K (Ref. 19).

A check for self-absorption was made by placing a mirror on the side of the flame opposite the spectrograph and observing the increase in intensity for radiation from the flame being reflected back through the flame and into the spectrograph. The change in self-absorption for the (0, 0) band over the flame region of interest was less than 3 percent. Since the measurements taken were only relative measurements, this change in self-absorption was considered negligible.

To prevent errors to the emission measurements due to reflectance from a cell window on the opposite side of the flame from the spectrograph, the window was covered with black felt while the emission measurements were made.

## 4.5 DESCRIPTION OF APPARATUS

### 4.5.1 UV Spectrometer

A 3/4-meter Czerny Turner grating spectrometer having an optical speed of f/6.8 and equipped with straight slits was used. The grating had 1180 lines/mm and was 104 by 104 mm in size. The detector used was a 1P28 photomultiplier tube. The external optics consisted of a 3.8-cm-diam fused silica lens with a focal length of 14 cm and a fused silica dove prism mounted so that a horizontal image on the flame was focused on the vertical slit of the spectrograph. This provided a spatial resolution along the flame axis of approximately 0.5 mm. This system was used for both the OH absorption measurements and the OH emission measurements from the flame. For the absorption measurements, a slit width of 0.015 mm and a slit height of 5 mm was used. For the emission measurements from the flame, a 0.2-mm slit width was required because of the low intenstiy of the flame emission.

### 4.5.2 IR Spectrometer

A Perkin-Elmer double-pass prism spectrometer equipped with an NaCl prism was used. The detector used was a lead sulfide cell. The external optics were identical with those used on the uv spectrograph. This system was used for the $H_2O$ emission and absorption measurements for use in calculating the temperature. A slit width of 300 $\mu$ and a slit height of 5 mm were used.

### 4.5.3 OH Source

A capillary, end view, water-cooled discharge tube was used to provide a narrow line source for the OH absorption measurements. The capillary was 15 cm long and 3 mm in diameter. It was surrounded by a water-cooling jacket. A fused silica window was installed at one end of the tube. Argon was bubbled through water and pulled through the tube by a vacuum pump. The tube was operated at a pressure of 8 mm Hg. The low pressure and water-cooled jacket combined to ensure a narrow emission line compared with the broad absorption line of the flame. A diagram of the discharge tube is shown in Fig. 14. A 2-cm-diam quartz lens with a focal length of 10 cm was used to focus the radiation from the tube to a point on the vertical axis of the flame.

### 4.5.4 Continuum Source

A Barnes blackbody simulator having an emissivity of 0.99 was used. It had a temperature range of from 200 to 1000°C. The source diameter

was 1.25 cm. A 3.8-cm-diam quartz lens with focal length of 14 cm was used to place an image of the source on the vertical axis of the flame.

#### 4.5.5 Burner

A water-cooled flat flame burner as shown in Fig. 15 was used. The top section of the burner consisted of a copper plate 1/2 in. thick with a square pattern of 1/16-in.-diam holes evenly spaced 1/8 in. apart. The flame was confined to a 3- by 2.8-cm center section of the burner face. This was surrounded by an $N_2$ sheath, 1 cm wide. A water-cooling passage lay just outside the sheath. The lower section of the burner consisted of a mixing chamber filled with copper shot as shown in Fig. 15. This burner produced a flame having a flat temperature profile for a distance of at least 6 cm downstream. At points above this distance, the profile began to round out somewhat but still remained relatively flat for a few more cm. All data taken in this study were in the 0- to 5-cm range. The burner was mounted on a vertical hydraulic jack in the test cell so that it might be positioned for measurements at various axial positions in the flame without moving the spectrometer.

#### 4.5.6 Gas Control and Measuring System

The gas flow measuring system consisted of a network of orifices and pressure transducers. The orifices were calibrated for volume flow of each gas of interest against upstream orifice pressure. The calibration was accomplished by flowing a gas through the orifice at a particular upstream pressure into a vacuum tank of known volume. The volume flow could then be accurately calculated by recording the rate of pressure change and the rate of temperature change in the vacuum tank and application of the equation,

$$V \frac{d\bar{P}}{dt} = \bar{R} T \frac{d\bar{n}}{dt} + n \bar{R} \frac{dT}{dt} \tag{51}$$

where V is the volume of the tank, $\bar{P}$ is the pressure, $\bar{R}$ is the universal gas constant, T is the temperature, t is the time, and $\bar{n}$ is the number of moles. It was found that the tank was large enough so that dT/dt was negligible and Eq. (51) reduced to

$$V \frac{d\bar{P}}{dt} = \bar{R} T \frac{d\bar{n}}{dt} \tag{52}$$

A schematic showing the arrangement of the gas control and measuring system as applied to each gas is shown in Fig. 16.

### 4.5.7 Test Cell

The test cell consists of a 12-in.-diam vertical steel duct with four circular ports of 6-in. diameter. It is connected to the main pumping system of the Rocket Test Facility and has the capability of operating at any pressure in the range from 0.5 to 760 mm Hg. For this study, the pressure was maintained at 380 mm Hg. This was found to be the best pressure for providing a steady flame so that the needed parameters could be accurately measured. A schematic of the test cell is shown in Fig. 17. A photograph showing the arrangement of the apparatus around the cell is presented in Fig. 18.

## SECTION V
## RESULTS AND DISCUSSION

### 5.1 BURNER CONFIGURATION EXPERIMENTS

Burners of different size and design were built and tested at various pressures in an attempt to produce a stabilized lean $H_2$-$O_2$ flame. The early experiments involved burners with porous plug faces such as that used by Kaskan (Ref. 9) for studies in rich flames. These were found unsatisfactory for the present study because of the low rise velocity of the flames and the instability of flames produced by them.

The next step was to use burners with faces made from thick metal plates containing many small holes. These burners were found to produce a fairly steady $H_2$-$O_2$-D flame. Without the diluent gas, the pure $H_2$-$O_2$ flames flashed back and burned inside the burner causing damage. The reason for the difference in the two flames may be attributed to the fact that the diluent gas reduces the flame velocity and results in a steady uniform flame. A modification which improved the stability of the lean flames was to lower the flame section of the burner slightly below the metal surface as shown in Fig. 16. This served as a place for the flame to attach and prevented flickering. Another modification over earlier burners was the use of a square pattern for the burner face. This improved the temperature profile of the flame and resulted in almost completely uniform temperature throughout the regions of interest.

The burner was operated in various pressure environments and was found to provide steady flames for the pressure range of from 200 to 760 mm Hg. Throughout the present study the burner was operated at 380 mm Hg.

## 5.2 FLAME EXPERIMENTS

### 5.2.1 Measurements

Measurements of gas temperature, OH concentration, and the band intensity in emission from the $A\ ^2\Sigma^+ \rightarrow X\ ^2\Pi_i$ (0, 0) transition of OH were made at various axial positions downstream of the reaction zone in six $H_2$-$O_2$-D flames resulting from premixed gases with different composition. The compositions, operating parameters, and results of OH concentration and temperature measurements are shown in Table II for the six flames investigated. The temperature as shown in the table was found to be constant throughout the region investigated. The rise velocity, ($\dot{X}$), which is the velocity at which the hot gases proceed downstream of the reaction zone, was calculated for each flame by measuring the input mass flows ($\dot{m}$) and using the mass conservation equation,

$$\rho A \dot{X} = \text{constant} \tag{53}$$

where $\rho$ is the gas density and A is the cross-sectional area of the flame. Since this was a one-dimensional constant pressure process, the velocity axial profile was constant downstream and could be calculated by the equation,

$$\dot{X} = \frac{\dot{m}}{\rho A} \tag{54}$$

### 5.2.2 Calculation of Species Concentration

Temperature and OH concentration measurements that were used to calculate the concentration of each species in the flame are listed in Table II. The diluent gas used in each flame did not enter into the reactions and could, therefore, be considered inert. This allowed a method to be developed for using $H_2$-$O_2$ flame tables combined with the measurements of temperature and OH concentration to find the concentration of each species in the flame. The species normally found in the $H_2$-$O_2$-D flame are $H_2$, $O_2$, H, O, OH, $H_2O$, and D. Photographs of the spectrum from 2700 to 5500 Å were made, and no evidence of impurities was found. The method for finding species concentration is described below.

The concentration of hydrogen atoms ($n_H$), whether present in the flame as free atoms or as a constituent of one of the species, may be written as

$$n_H = 2[H_2O] - 2[H_2] + [OH] - [O] \tag{55}$$

The concentration of oxygen atoms ($n_O$) may be written as

$$n_O = [H_2O] + 2[O_2] + [OH] + [O] \tag{56}$$

The ratio of the number of diluent gas molecules to the number of hydrogen atoms ($n_H$) may be written

$$\frac{[D]}{n_H} = R \tag{57}$$

where R may be found from knowledge of input flows and is given by

$$R = \frac{\text{Volume Flow Rate of D}}{2 \times \text{Volume Flow Rate of } H_2} \tag{58}$$

Combining Eqs. (55) and (57) gives

$$[D] = R\,[2[H_2O] + 2[H_2] + [OH] + [H] \tag{59}$$

The concentration of all molecules (n) in the flame may be written as

$$n = [D] + n\,[f_{H_2O} - f_{OH} - f_{H_2} - f_{O_2} - f_H - f_O] \tag{60}$$

where the f's are the various species mole fractions. The value of the number density of molecules (n) may be calculated from the ideal gas law

$$n = \frac{\bar{P}\,N}{\bar{R}\,T} \tag{61}$$

where $\bar{P}$ is the pressure, N is Avogardro's number, $\bar{R}$ is the universal gas constant, and T is the temperature.

To use the values of mole fractions as found in equilibrium tables, Eq. (60) must be rewritten to account for the dilution of the flame by D. This results in the equation,

$$n = [D] - C\,[f'_{H_2O} - f'_{OH} + f'_{H_2} - f'_{O_2} - f'_H - f'_O] \tag{62}$$

where C is now an unknown less than n and the f's are pseudo mole fractions and are the true mole fractions that would be found in an

$H_2$-$O_2$ flame if [D] = 0. Since $H_2O$ and $O_2$ are considered to be at their equilibrium values throughout the recombination zone, their pseudo mole fraction may be taken from equilibrium tables. The tables used in this study were compiled by Svehla (Ref. 20). The values of the other species must be handled differently since they are not necessarily in equilibrium concentrations. From Eq. (62), it is seen that

$$[M] = Cf'_m \tag{63}$$

for each of the species. Combining this with the equilibrium Eqs. (10) through (12) gives

$$f'_H = \frac{[H]}{C} = K_H \frac{[OH]^3}{C^3 f'_{H_2O} f'_{O_2}} \tag{64}$$

$$f'_{H_2} = \frac{[H_2]}{C} = K_{H_2} \frac{[OH]^2}{C^2 f'_{O_2}} \tag{65}$$

$$f'_O = \frac{[O]}{C} = K_O \frac{[OH]^2}{C^2 f'_{H_2O}} \tag{66}$$

and

$$f'_{OH} = \frac{[OH]}{C} \tag{67}$$

By using Eq. (63), Eq. (59) can be rewritten as

$$[D] = R\,C\,[2 f'_{H_2O} + 2 f'_{H_2} + f'_{OH} - f'_H] \tag{68}$$

Combining this with Eq. (62) results in

$$n = C\,[(2R + 1) f'_{H_2O} + (2R + 1) f'_{H_2} + (R + 1) f'_{OH} + (R + 1) f'_H + f'_{O_2} + f'_O] \tag{69}$$

Substituting into Eq. (69) the expressions found for $f'_H$, $f'_{H_2}$, $f'_O$, and $f'_{OH}$ in Eqs. (64) through (67), then substituting into the resulting equation the values for the pseudo mole fractions of $H_2O$ and $O_2$ found in the equilibrium tables, multiplying through by $C^2$, and rearranging

terms yield the result

$$C^3 [(2R + 1) f'_{H_2O} + f'_{O_2}] - C^2 [n - (R + 1) [OH]]$$

$$+ \left[ (2R - 1) K_{H_2} \frac{[OH]^2}{f'_{O_2}} + K_O \frac{[OH]^2}{f'_{H_2O}} \right]$$

$$+ (R + 1) K_H \frac{[OH]^3}{f'_{H_2O} f'_{O_2}} = 0 \qquad (70)$$

Equation (70) is then solved for C, and by using Eqs. (63) through (67), the concentration of each species may be found. This procedure was written as a computer program and is included here as Appendix III.

This procedure is applicable for flames with temperatures below 2500°K. For these temperatures, the equilibrium mole fractions of $H_2O$ and $O_2$ are not significantly affected by the presence of the diluent. For higher temperatures, the equilibrium mole fractions are noticeably affected by the diluent, and the calculation of species concentrations requires an iterative process as developed by Peters, Peters, and Billings (Ref. 21).

Calculations of the species concentrations were made, using the method described above, from measurements of OH concentration and temperature at various axial stations downstream of the reaction zone for each of the six flames listed in Table II. The results of the subsequent calculations for the six flames are shown in Table III. The time shown in the table and in later figures is the time downstream of the reaction zone and is found by dividing the position above the burner where the measurement was made by the rise velocity of the flame.

#### 5.2.3 Determination of Chemiluminescence

If the absolute value of the total OH radiation due to $A\ ^2\Sigma^+ \rightarrow X\ ^2\Pi_i$ (0, 0) transitions were known, then radiation due to chemical reactions ($Q_{ch}$) could be found in a straightforward manner from Eq. (20). The intensity of OH radiation from lean flames is too small to allow measurement of the structure of the band, and the band is overlapped by other bands. Therefore, the absolute value of the total radiation cannot be measured directly, and a method of fitting curves based on the theory must be used.

The total measured relative radiation (Q) is made up of two parts, thermal and chemiluminescent. This may be written as

$$^{i}Q = {}^{i}Q_{ch} + {}^{i}Q_{th} \tag{71}$$

where the superscript (i) designates a particular station along the axis of the flame. Although the absolute value of Q is not known, relative values at different stations in the flame may be compared. In Fig. 19, values at time $t_1$ and $t_2$ are compared, with their ratio being

$$\frac{^{1}Q}{^{2}Q} = \frac{^{1}Q_{ch} + {}^{1}Q_{th}}{^{2}Q_{ch} + {}^{2}Q_{th}} \tag{72}$$

An absolute value for the thermal radiation may be found using Eq. (19). Since the upper state is a $^2\Sigma$ state, its statistical weight ($g_e$) is 2. The vibrational statistical weight ($g_v$) is unity. The electronic partition function $(p.f.)_e$ is given by

$$(p.f.)_e = \sum_n g_e\, e^{-E_n/kT} \tag{73}$$

which for OH is 4. The vibrational partition function $(p.f.)_v$ for the $A\,^2\Sigma^+$ state is given by

$$(p.f.)_v = \sum_v e^{-G(v)/kT} \tag{74}$$

where G(v) is the vibrational energy for the energy state whose vibrational quantum number is v. The vibrational partition function is shown as a function of temperature in Fig. 20. The electronic term level energy for the $^2\Sigma$ state of OH is given in Herzberg (Ref. 15) and has a value of 32682 $cm^{-1}$. The transition probability (A) is that found by Broida and Carrington (Ref. 22) and has a value of $1.05 \times 10^6$ $sec^{-1}$. If these values are substituted into Eq. (19), the result is

$$Q_{th} = \frac{0.525 \times 10^{6}}{(p.f.)_v}\,[OH]_e\, e^{-\frac{4.7 \times 10^{4}}{T}}\ \frac{\text{photons}}{\text{sec-cm}^3} \tag{75}$$

From the measurements of OH concentration and temperature as given in Tables II and III, absolute values of $Q_{th}$ may be calculated for different points in the stream, in particular, at times $t_1$ and $t_2$. These values may now be substituted into Eq. (72).

In Eq. (14), it is seen that, if the theory is correct, $Q_{ch}$ should be proportional to the fifth power of the OH concentration. This may be written as

$$^{i}Q_{ch} \propto {}^{i}[OH]^{5} \tag{76}$$

Although the absolute value of $Q_{ch}$ is not known, relative values at different stations in the flame may be compared. In particular, values at times $t_1$ and $t_2$ may be compared by using the values for OH concentration found in Table III. Their ratio is

$$\frac{^{1}Q_{ch}}{^{2}Q_{ch}} = \frac{^{1}[OH]^{5}}{^{2}[OH]^{5}} \tag{77}$$

Equations (72) and (77) can be solved simultaneously to find absolute values for $^{1}Q_{ch}$ and $^{2}Q_{ch}$. By using Eq. (71), an absolute value can now be assigned to the measured total radiation curve. If the total radiation curve and the calculated thermal radiation curve are plotted in absolute units as functions of time, the chemiluminescent radiation as a function of time is given by the differences in the two curves. This is illustrated in Fig. 21. The results of applying this method to the six flames used in this study are shown in Fig. 22.

Theory predicts that a plot of log $Q_{ch}$ versus log [OH] should result in a straight line with a slope of 5. Such plots were made for each flame, using Fig. 22 to find the values of $Q_{ch}$ and using Table III to find the corresponding value of [OH]. The results appear in Fig. 23, where straight lines having a slope of 5 are shown with the experimental data points. Since for each flame the experimental data fit the theory quite well, it appears that the original assumption of partial equilibrium is valid for the flames involved. It should be noted that emission measurements were greater than predicted by this theory near the reaction zone. This is consistent with the results of Kaskan (Ref. 7) in rich flames and is to be expected for two reasons. One, the partial equilibrium concept is not valid in the reaction zone, and two, it is thought that a different excitation process may be taking place in the reaction zone (Ref. 19).

#### 5.2.4 Choice of Reaction

As may be seen in Fig. 23, the chemiluminescent radiation from a lean flame is at the most only a few times greater than that expected thermally. To obtain a straight line for a plot of log $Q_{ch}$ versus log [OH], a compensation had to be made for the thermal radiation. In a rich flame, the OH radiation is much greater than the thermal radiation, and such a

compensation was not necessary. This is illustrated in Fig. 6, in which Kaskan shows that a straight line plot is obtained for intensity versus |OH| on log-log paper without compensating for the thermal radiation. Attempts to show the 5th power dependence for lean flames using the data obtained in this study resulted in plots with curvature.

The fact, established by data obtained in this study, that OH chemiluminescent radiation is less intense in lean $H_2$ flames than in rich flames can be used to narrow the identification of the reaction responsible for the excess excitation of OH. The kinetic rate equations for each of the Reactions (IX) through (XII) are

$$\frac{d[OH]^*}{dt} = K_{IX}[H][OH]^2 \tag{78}$$

$$\frac{d[OH]^*}{dt} = \sum_m k_{mX}[O][H][M] \tag{79}$$

$$\frac{d[OH]^*}{dt} = k_{XI}[O][H_2][OH] \tag{80}$$

$$\frac{d[OH]^*}{dt} = k_{XII}[H][O_2][H_2] \tag{81}$$

For Reaction (IX), excitation would occur much more often in rich flames, where |H| is larger than in lean flames. For Reaction (X), excitation would occur at about the same rate in rich and lean flames because [O] is very small in rich flames, whereas [H] is very small in lean flames. For Reaction (XI), excitation would occur at about the same rate in rich and lean flames because [O] is very small in rich flames and $[H_2]$ is very small in lean flames. For Reaction (XII), excitation would occur much more often in rich flames, where both [H] and $[H_2]$ are large and only $[O_2]$ is small; whereas in lean flames, both [H] and $[H_2]$ are small and $[O_2]$ is large.

The only reactions which can explain the experimental data are, therefore, Reactions (IX) and (XII). Wolfhard[1] stated that all efforts to measure directly the preassociation phenomena, which he and Gaydon (Ref. 4) proposed for excitation of OH to the v = 2 and 3, $^2\Sigma$ levels of OH, had met with failure. Recent experiments (Ref. 19) in which excitation of the (0, 0), (2, 1), and (3, 2) bands of OH were examined at various

[1]Conversation with H. G. Wolfhard, AEDC, 1957.

pressures in $H_2$-$O_2$ flames, showed that the preassociation reaction, Reaction (III), contributes little if any to the excitation of the OH and that one of the three-body reactions must be responsible. This was reasoned from their results on the measurements at various pressures. They proposed that at low pressures the two-body preassociation reaction should predominate over any three-body reaction. Since the preassociation reaction can excite the OH radical to only the higher vibrational levels, 2 and 3, these levels should show stronger excitation relative to the v = 0 level than would be found at higher pressures. The experiments showed that such a preference did not exist. Instead, the excitation to each level remains essentially the same, relative to one another, at both atmospheric and low pressures.

From these results, the only conclusion is that the reaction responsible for the OH excitation must be one of the three-body reactions which is sufficiently exothermic so as to excite OH to each of the upper vibrational levels from v = 0 to v = 3. Examination of Table I shows that, of the two Reactions (IX) and (XII), only (IX) supplies the necessary additional energy for excitation to the higher vibrational levels. Therefore, the excitation reaction responsible for the OH excitation has been narrowed to Reaction (IX).

#### 5.2.5 Calculation of the Excitation Reaction Rate of OH

Now that the excitation reaction has been found, Eq. (20) may be rewritten as

$$Q_{ch} = \frac{A}{A + \sum_m k_{-m}[M]} K_{IX}[H][OH]^2 \tag{82}$$

This can be solved for $K_{IX}$ and results in

$$K_{IX} = \frac{A + \sum_m k_{-m}[M]}{A} \frac{Q_{ch}}{[H][OH]^2} \tag{83}$$

Since values of $Q_{ch}$ as functions of [OH] for each flame are available from Fig. 23 and the value of species concentrations have been found for each flame for each measured value of [OH] , knowledge of the quenching rates ($k_{-m}$) would allow calculation of the excitation reaction rate ($K_{IX}$) for each flame.

Values of the quenching rates were taken from data given by Hooymayers and Alkemade (Ref. 23), who measured the resonance yield factor (p) for the $^2\Sigma$ - $^2\Pi$ (0, 0) transition of OH in several $H_2$-$O_2$-D

flames. By comparing measurements in various flames of different composition, they were able to calculate the quenching rates for each species in the flame. Table IV (Ref. 23) shows the flame composition, temperatures, and measured resonance yield factors for the flames used in the study and the calculated quenching rates for the predominant species in the flames. Quenching rates are essentially temperature independent (Ref. 24), and these results may be applied to the data found in this study. Actually, the temperatures of the flames used in Hooymayers and Alkemade's measurements are similar to the flame temperatures of this study. For $H_2$ lean flames, it is evident that the only species with large enough concentrations to affect the quenching of OH are $H_2O$, $O_2$, and D. A value of $Q_{ch}$ and the corresponding values of [H], [OH], $[H_2O]$, $[O_2]$, and [D] for each flame were substituted into Eq. (83) along with the values of $k_{-m}$ from Table IV, and a value for $K_{IX}$ was found.

The radiative excitation reaction rate ($pK_{IX}$) was calculated for each flame. This is the constant that, when multiplied by the concentration of the species involved in the reaction, gives the number of quanta per second which will be emitted as a result of the chemical excitation. The values of $K_{IX}$, $pK_{IX}$, and p for each flame are shown in Table V.

#### 5.2.6 Measurements of the Excitation Rate

Three-body reactions are almost completely independent of temperature (Ref. 24). Therefore, the values of the excitation rates ($K_{IX}$) should be approximately the same for each of the six flames. The average value of $K_{IX}$ was found to be $2.3 \times 10^{-32}$ $cm^6$-molecule$^{-2}$ $sec^{-1}$, and its standard deviation was found to be $0.9 \times 10^{-32}$ $cm^6$-molecule$^{-2}$ $sec^{-1}$. The results may be compared with those found by Kaskan (Ref. 7) in rich $H_2$-$O_2$-$N_2$ flames. He estimated a value for $K_{IX}$ to be approximately $3 \times 10^{-32}$ $cm^6$-molecules$^{-2}$ $sec^{-1}$. His estimate was based on a larger value of A of $1.7 \times 10^6$ $sec^{-1}$ and the assumption that all species in the flame had equal quenching efficiency.

## SECTION VI
## CONCLUSIONS AND PROJECTIONS FOR FUTURE STUDIES

In this study, a method has been outlined for investigating extrathermal radiation from flames. In the case of chemiluminescence, a method of approach for isolating the chemical reactions responsible was shown. A method for calculating the excitation reaction rate of such a

reaction was developed. For the OH radical, the excitation reaction was found to be

$$OH + OH + H \xrightarrow{K_{IX}} OH^* + H_2O$$

and the rate of excitation ($K_{IX}$) was found to be $(2.3 \pm 0.9) \times 10^{-32}$ $cm^6$-molecule$^{-2}$-sec$^{-1}$. Although this study was confined to the OH radical, the methods developed could be extended to other species which are known to be chemiluminescent in nature. These include NH, CN, Na, K, Li, and many others.

An indirect result of this study was the conclusion that the concept of partial equilibrium is valid for lean $H_2$-$O_2$ flames downstream of the reaction zone. This supports the belief of many investigators in reaction kinetics.

Additional experimental and theoretical work in the study of the chemiluminescent phenomena would be extremely valuable in advancing basic knowledge of flame radiation processes. Measurements of the excitation rates for other bands of OH might be the next logical step to take. From there, the probelm of measurements of rates for chemiluminescent excitation of NH and CN might be attacked. Each of these measurements requires many experimental preludes including finding the appropriate transition probabilities and the quenching rates by predominant species in the flame. As each of these variables is found, it will add to the knowledge necessary for predicting the intensity and the nature of the radiation resulting from chemical reactions in flames.

## REFERENCES

1. Kondratiev, V. and Ziskin, M. "The Spectrum of the Hydrogen Flames." Acta Physica et Chemica (USSR), Vol. 7, No. 1, January 1937, p. 65.

2. Gaydon, A. G. and Wolfhard, H. G. "Spectroscopic Studies of Low-Pressure Flames; Temperature Measurements in Acetylene Flames." Proceedings of the Royal Society of London, Vol. A194, No. 1037, August 1948, pp. 169-184.

3. Gaydon, A. G. and Wolfhard, H. G. "Spectroscopic Studies of Low-Pressure Flames V. Evidence for Abnormally High Electronic Excitation." Proceedings of the Royal Society of London, Vol. A205, No. 1080, January 1951, pp. 118-134.

4. Gaydon, A. G. and Wolfhard, H. G. , "Predissociation in the Spectrum of OH; the Vibrational and Rotational Intensity Distribution in Flames." Proceedings of the Royal Society of London, Vol. A208, No. 1092, August 1951, pp. 63-75.

5. Bulewicz, E. M., James, C. G., and Sugden, T. M. "Photometric Investigations of Alkali Metals in Hydrogen Flame Gases." Proceedings of the Royal Society of London, Vol. A235, No. 1200, April 1956, pp. 89-106.

6. Charton, M. and Gaydon, A. G. "Excitation of Spectra of OH in Hydrogen Flames and Its Relation to Excess Concentration of Free Atoms." Proceedings of the Royal Society of London, Vol. A245, No. 1240, May 1958, pp. 84-92.

7. Kaskan, W. E. "Abnormal Excitation of OH in $H_2/O_2/N_2$ Flames." Journal of Chemical Physics, Vol. 31, No. 4, October 1959, pp. 944-956.

8. Ellis, G. E. "Literature Survey of the Kinetics of the H-O-N System." MR 20-202, The Marquardt Corporation, November 1962.

9. Kaskan, W. E. "Hydroxyl Concentrations in Rich Hydrogen-Air Flames Held on Porous Burners." Combustion and Flame, Vol. 2, No. 3, July 1958, p. 229.

10. Kaskan, W. E. "The Concentration of Hydroxyl and of Oxygen Atoms in Gases from Lean Hydrogen-Air Flames." Combustion and Flame, Vol. 2, No. 3, July 1958, p. 286.

11. Getzinger, R. W. and Schott, G. L. "Kinetic Studies of Hydroxyl Radicals in Shock Waves V. Recombination via the $H + O_2 + M \rightarrow HO_2 + M$ Reaction in Lean Hydrogen-Oxygen Mixtures." Journal of Chemical Physics, Vol. 43, No. 9, November 1965, pp. 3237-3247.

12. Mitchell, A. C. G. and Zemansky, M. W. Resonance Radiation and Excited Atoms. The MacMillan Company, New York, 1934.

13. Penner, S. S. Quantitative Molecular Spectroscopy and Gas Emissivities. Addison-Wesley Publishing Company, Inc., Reading, Massachusetts, 1959.

14. Oldenberg, O. and Rieke, F. F. "Kinetics of OH Radicals as Determined by Their Absorption Spectrum." Journal of Chemical Physics, Vol. 6, No. 1, January 1938, p. 439.

15. Herzberg, G. Spectra of Diatomic Molecules. van Nostrand Company, Inc., New York, 1950. (Second Edition)

16. Dieke, S. H. and Crosswhite, H. M. "The Ultraviolet Bands of OH." Journal of Quantitative Spectroscopy and Radiative Transfer, Vol. 2, No. 4, April 1962, p. 97.

17. Learner, R. C. M. "The Influence of Vibration-Rotation Interaction on Intensities in the Electronic Spectra of Diatomic Molecules." Proceedings of the Royal Society of London, Vol. A269, No. 1338, September 1962, p. 311-325.

18. Brewer, L. E., Jr. and McGregor, W. K., Jr. "Experimental Determination of a Rocket Exhaust Gas Temperature at Altitude by Infrared Spectroscopy." AEDC-TN-61-94 (AD325076), September 1961.

19. Hinck, E. C., Seamans, T. F., Vanpee, M., and Wolfhard, H. G. "The Nature of OH Radiation in Low-Pressure Flames." Tenth Symposium (International) on Combustion, The Combustion Institute, 1965.

20. Svehla, R. A. "Thermodynamic and Transport Properties for the Hydrogen-Oxygen System." NASA SP-3011, 1964.

21. Peters, C. E., Peters, T., and Billings, R. B. "Mixing and Burning of Bounded Coaxial Streams." AEDC-TR-65-4 (AD458348), March 1965.

22. Broida, H. P. and Carrington, T. "Fluorescence and Average Lifetime of Excited OH ($^2\Sigma^+$) in Flames." Journal of Chemical Physics, Vol. 23, No. 11, November 1955, p. 2202.

23. Hooymayers, H. P. and Alkemade, C. T. J. "Quenching of Excited Hydroxyl ($^2\Sigma^+$, $v' = 0$) Radicals in Flames." Journal of Quantitative Spectroscopy and Radiative Transfer, Vol. 7, No. 3, May 1967, pp. 495-504.

24. Fristrom, R. M. and Westenberg, A. A. Flame Structure. McGraw-Hill Book Company, Inc., New York, 1965.

## APPENDIXES

I. ILLUSTRATIONS
II. TABLE
III. COMPUTER PROGRAM FOR CALCULATING SPECIES CONCENTRATIONS IN LEAN $H_2-O_2-D$ FLAMES

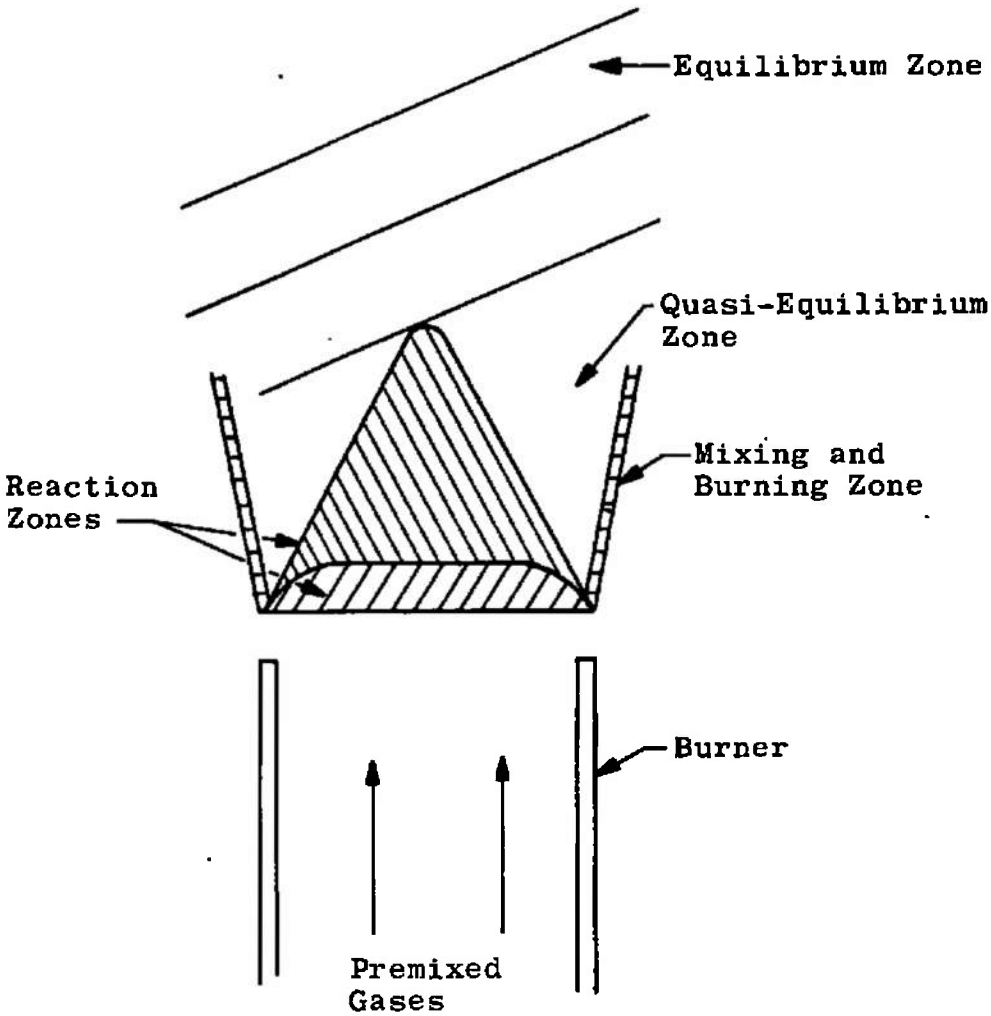


Fig. 1 Type of Flame Used in Early Studies

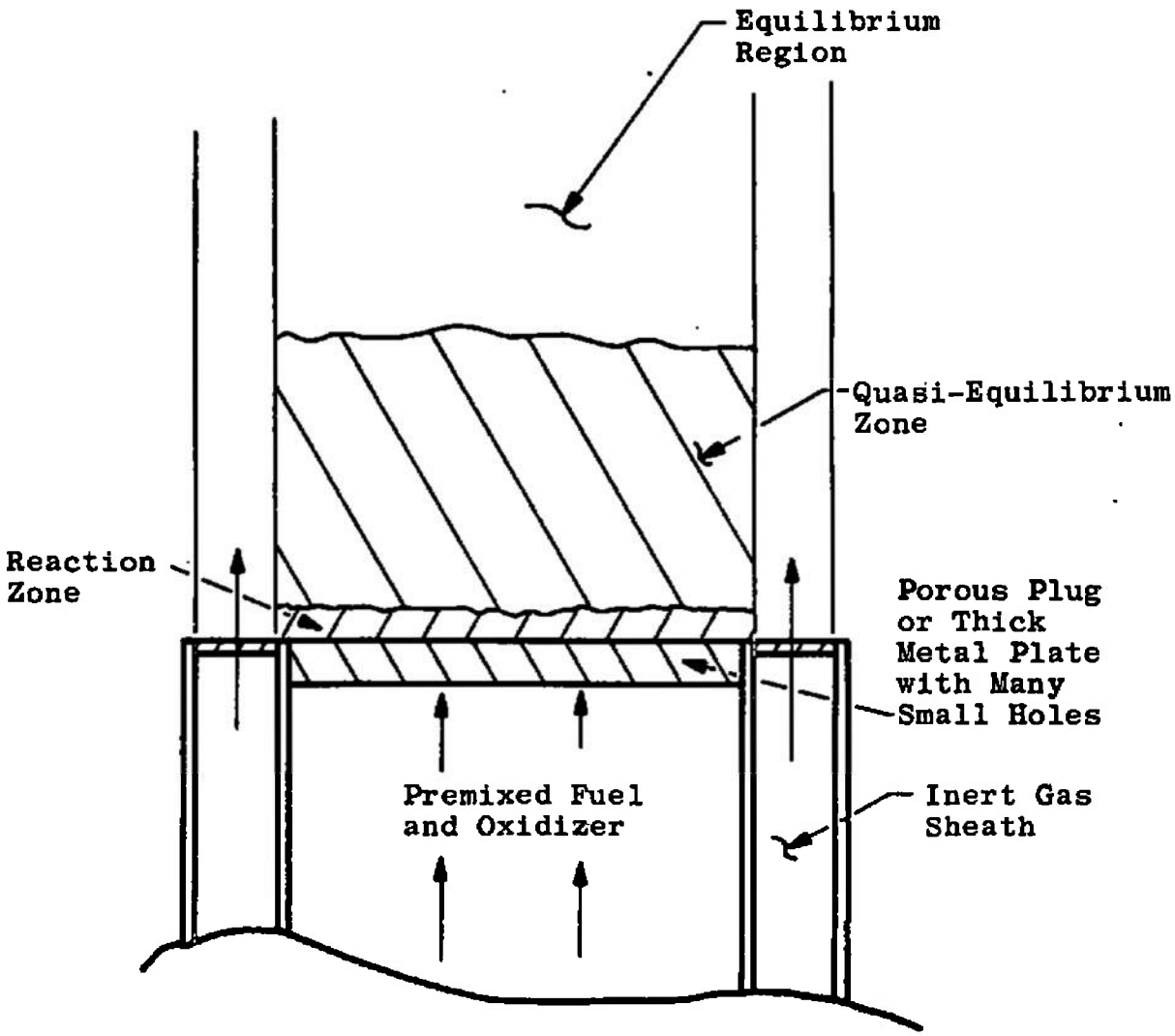


Fig. 2 Type of Flame Obtained on Flat Flame Burners

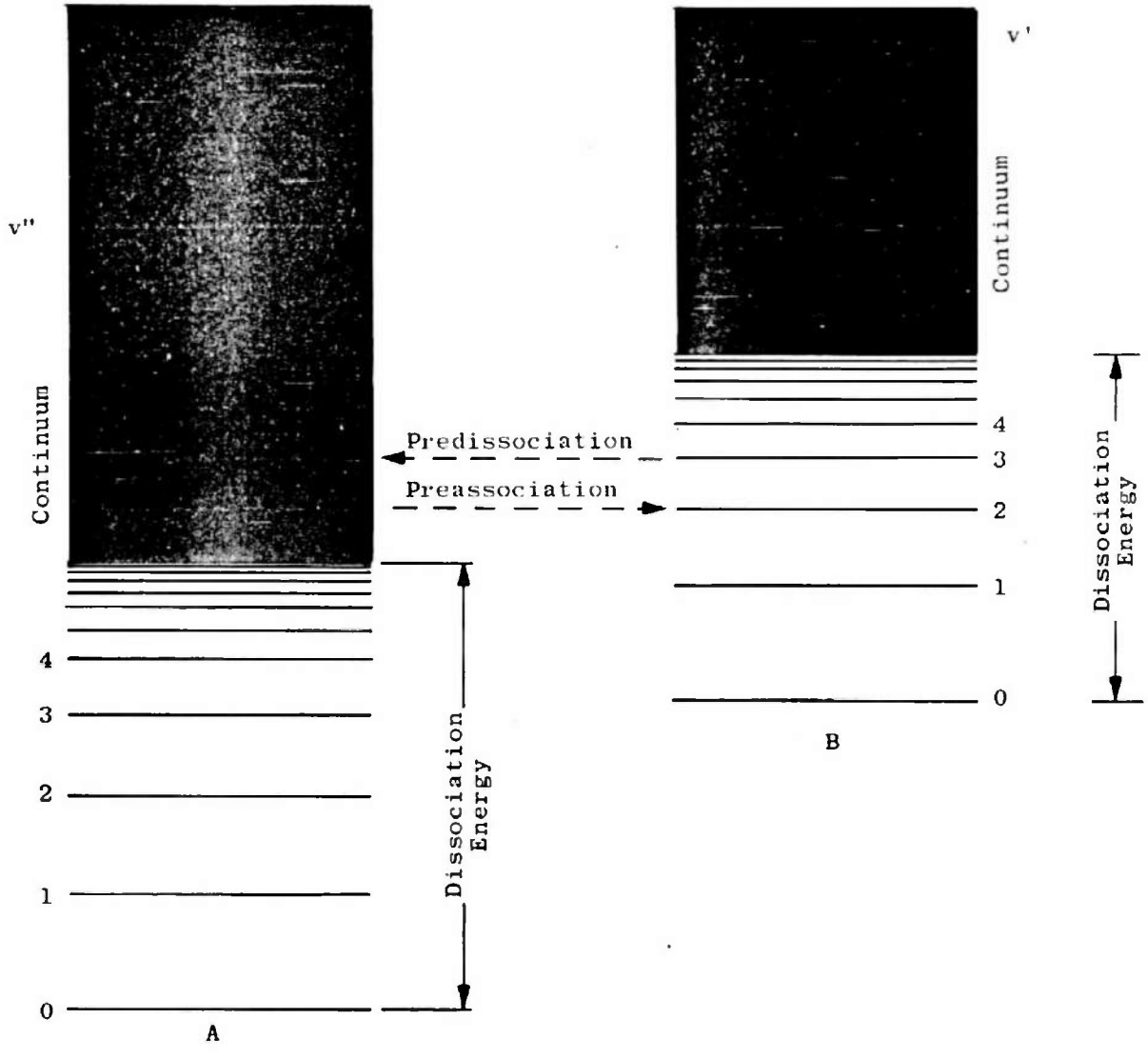


Fig. 3 Example of Preassociation and Predissociation between the Electronic States, A and B, of a Molecule

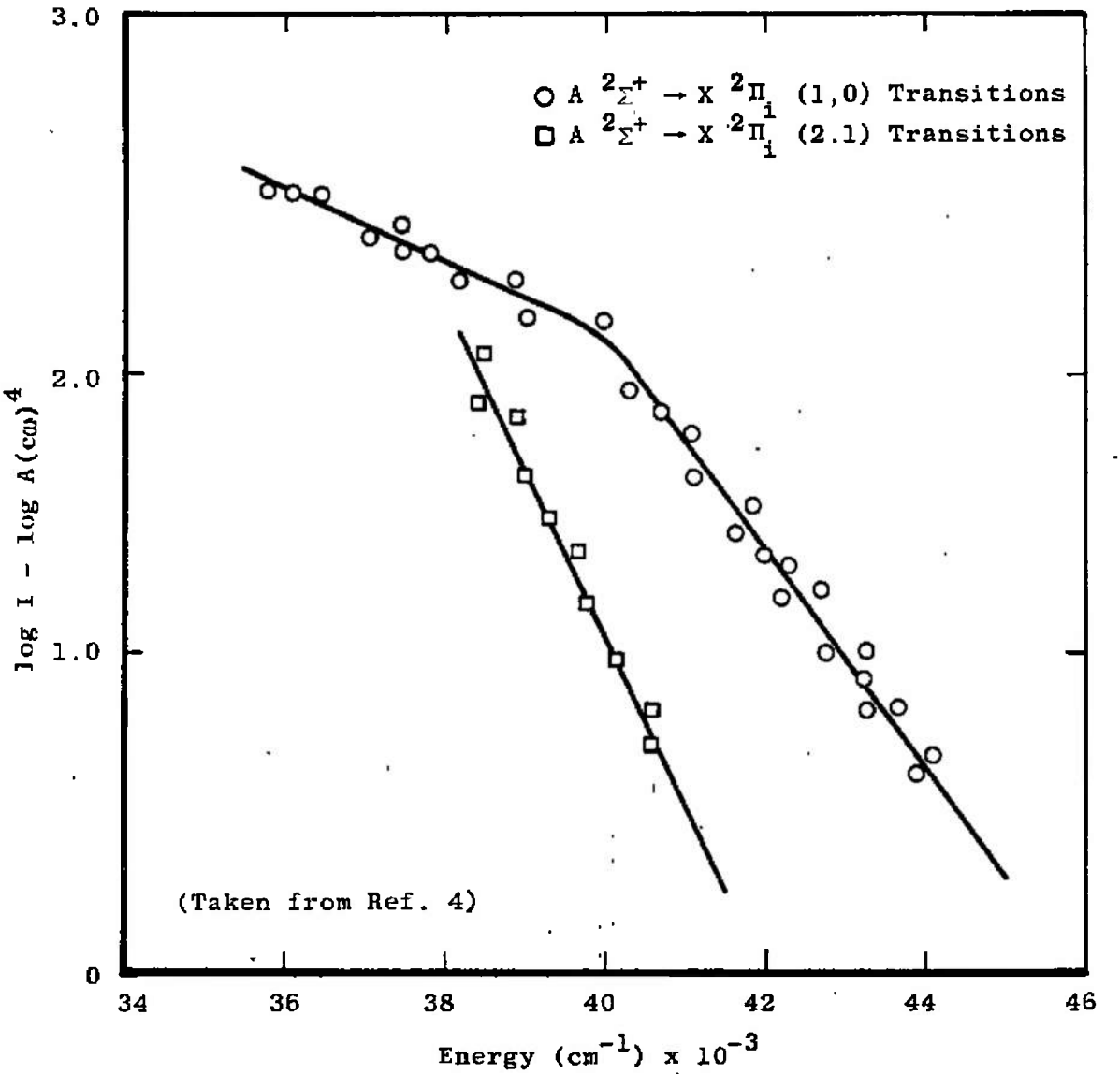


Fig. 4 Effect of Predissociation on the Spectra of OH in a Low-Pressure Acetylene-Air Flame

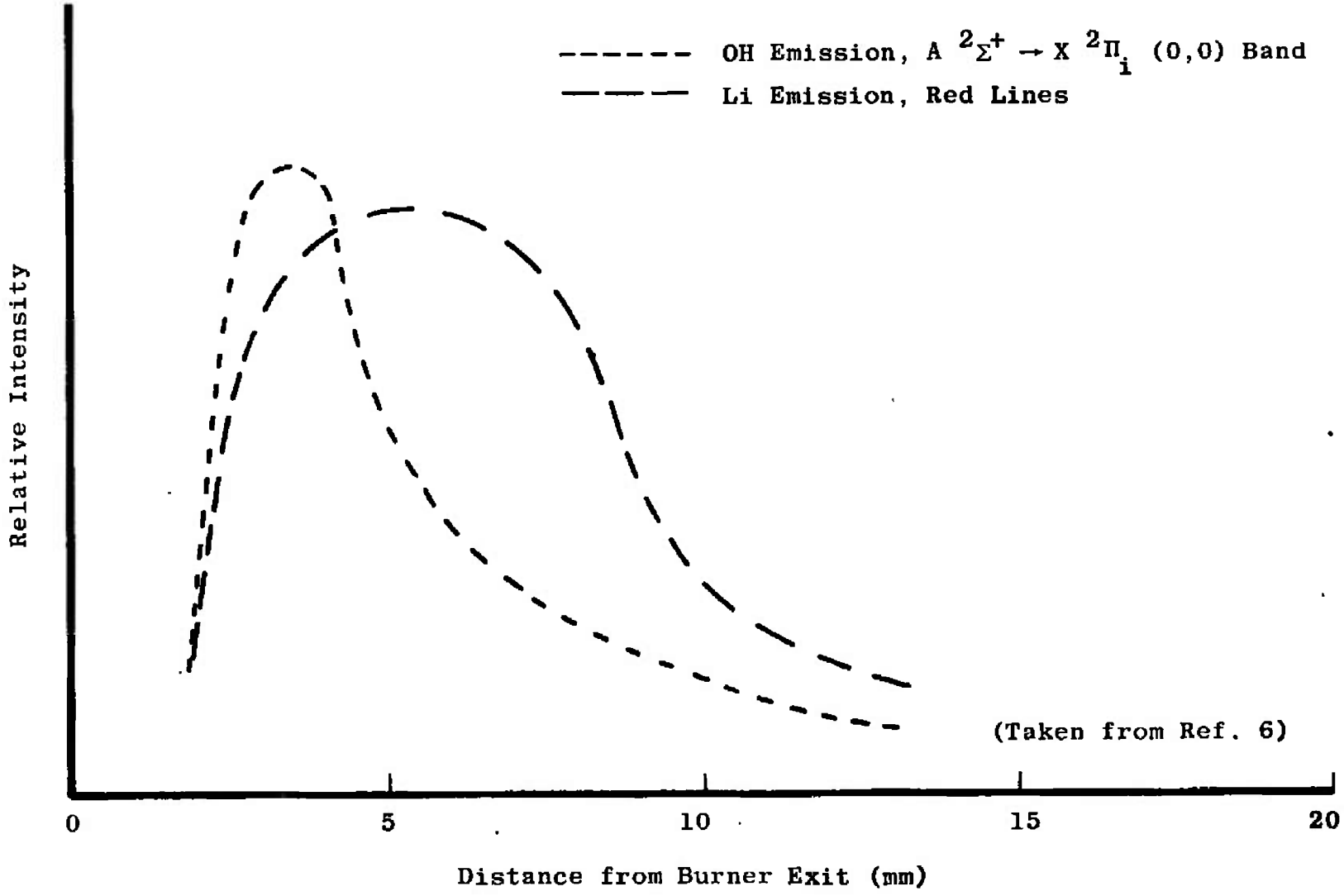


Fig. 5 Relative Intensities of OH and Li Radiation versus Height above Burner in a $H_2$–$O_2$–$N_2$ Flame

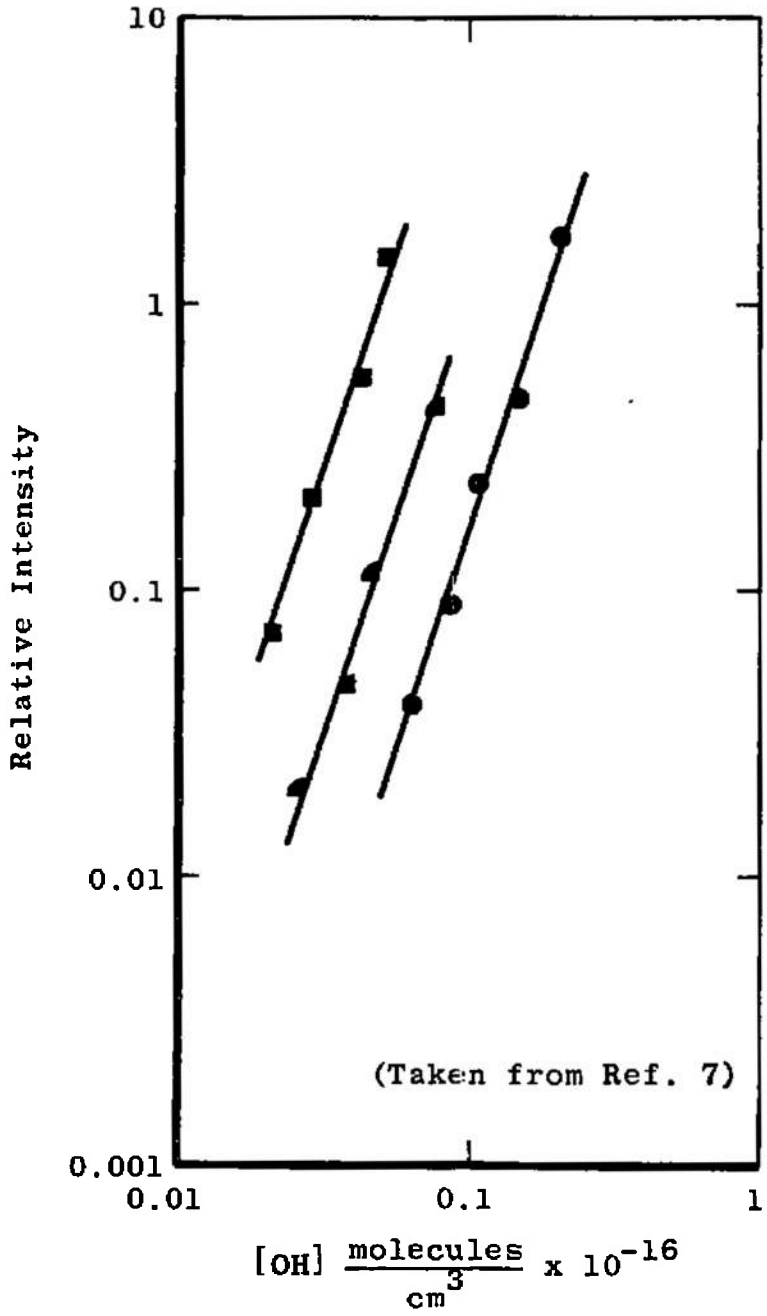


Fig. 6 Intensity of A $^2\Sigma \rightarrow X\ ^2\Pi_i$ (0,0) Band of OH as a Function of [OH] for Three Rich Flames with Different Fuel-Oxidizer Ratios

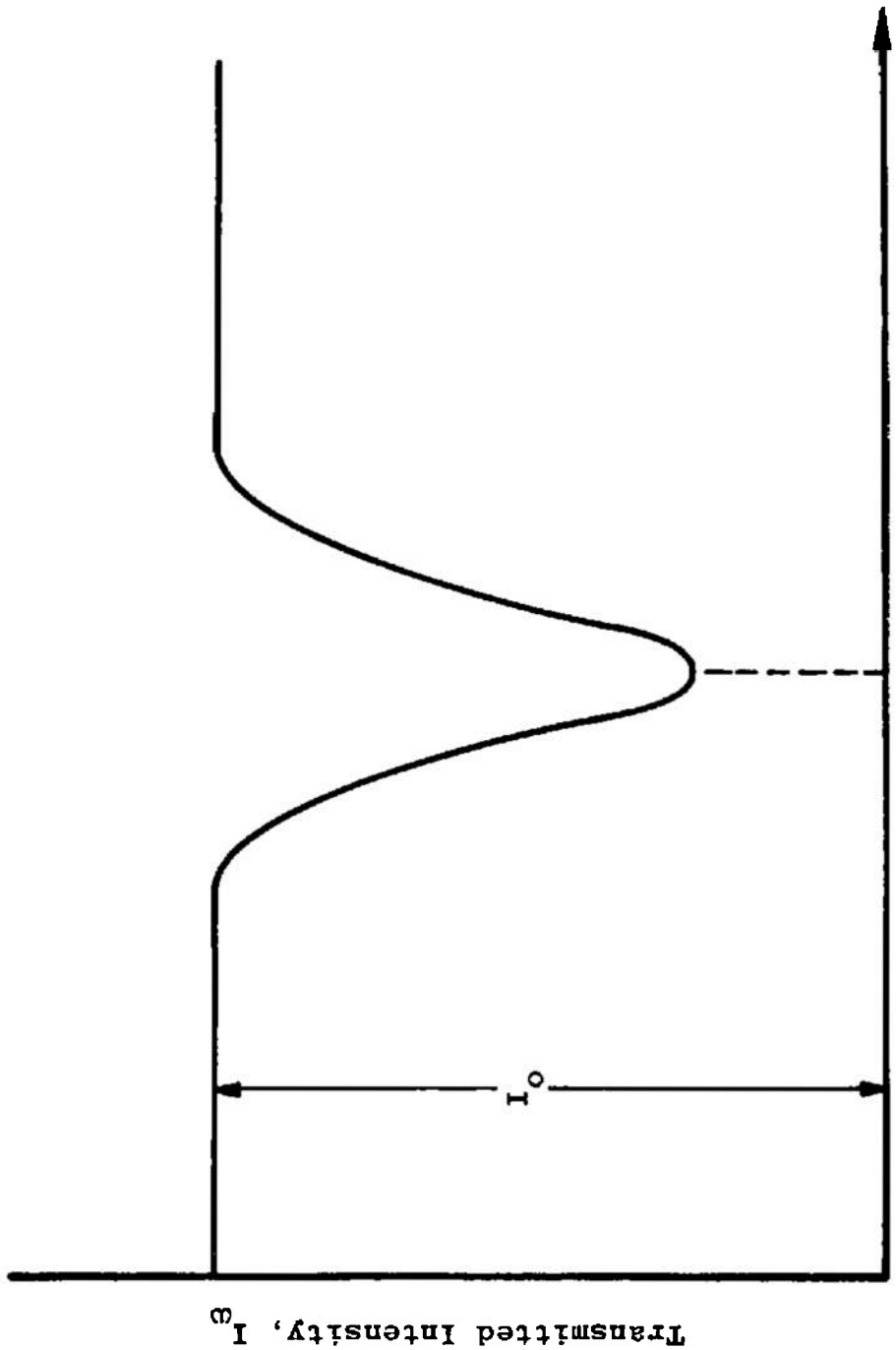


Fig. 7 Transmitted Intensity of Beam of Light as a Function of Wave Number for a Typical Spectral Absorption Line

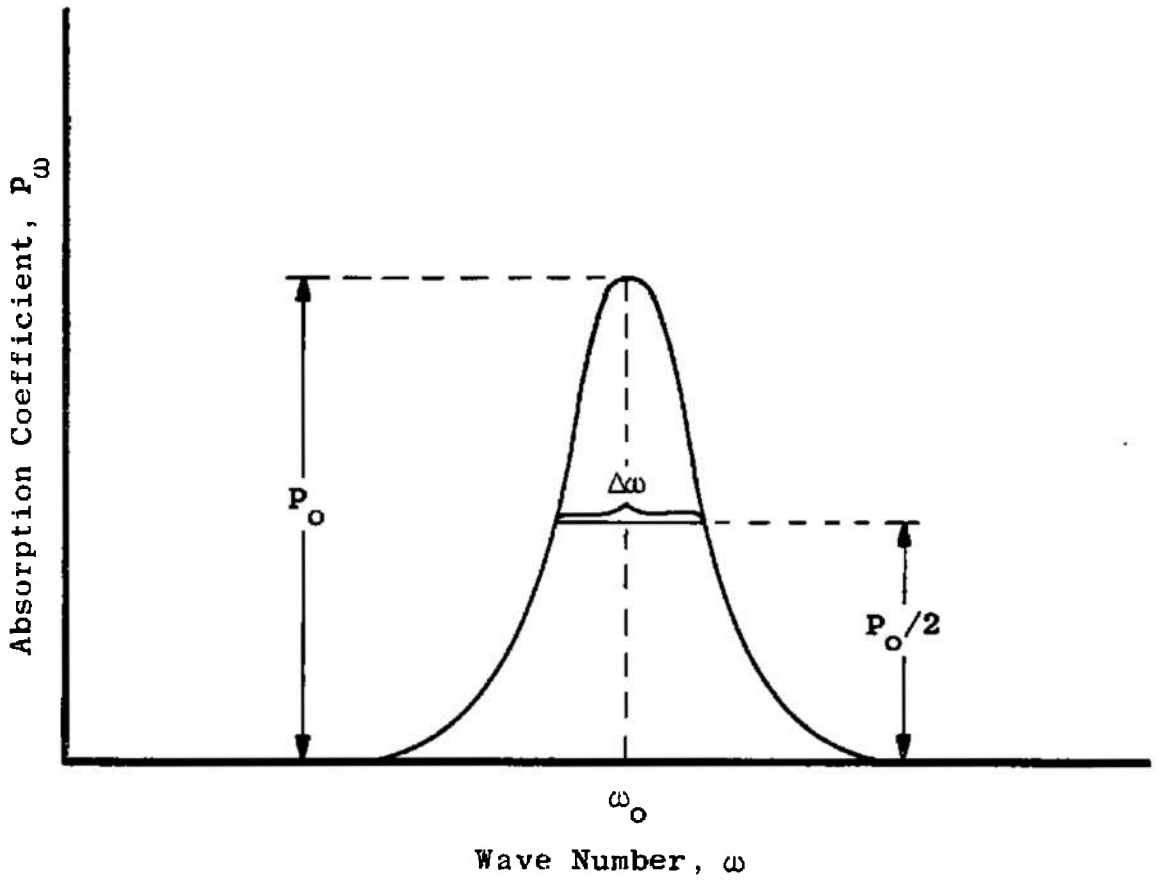


Fig. 8 Absorption Coefficient, $P_\omega$, as a Function of Wave Number, $\omega$, for a Typical Spectral Absorption Line

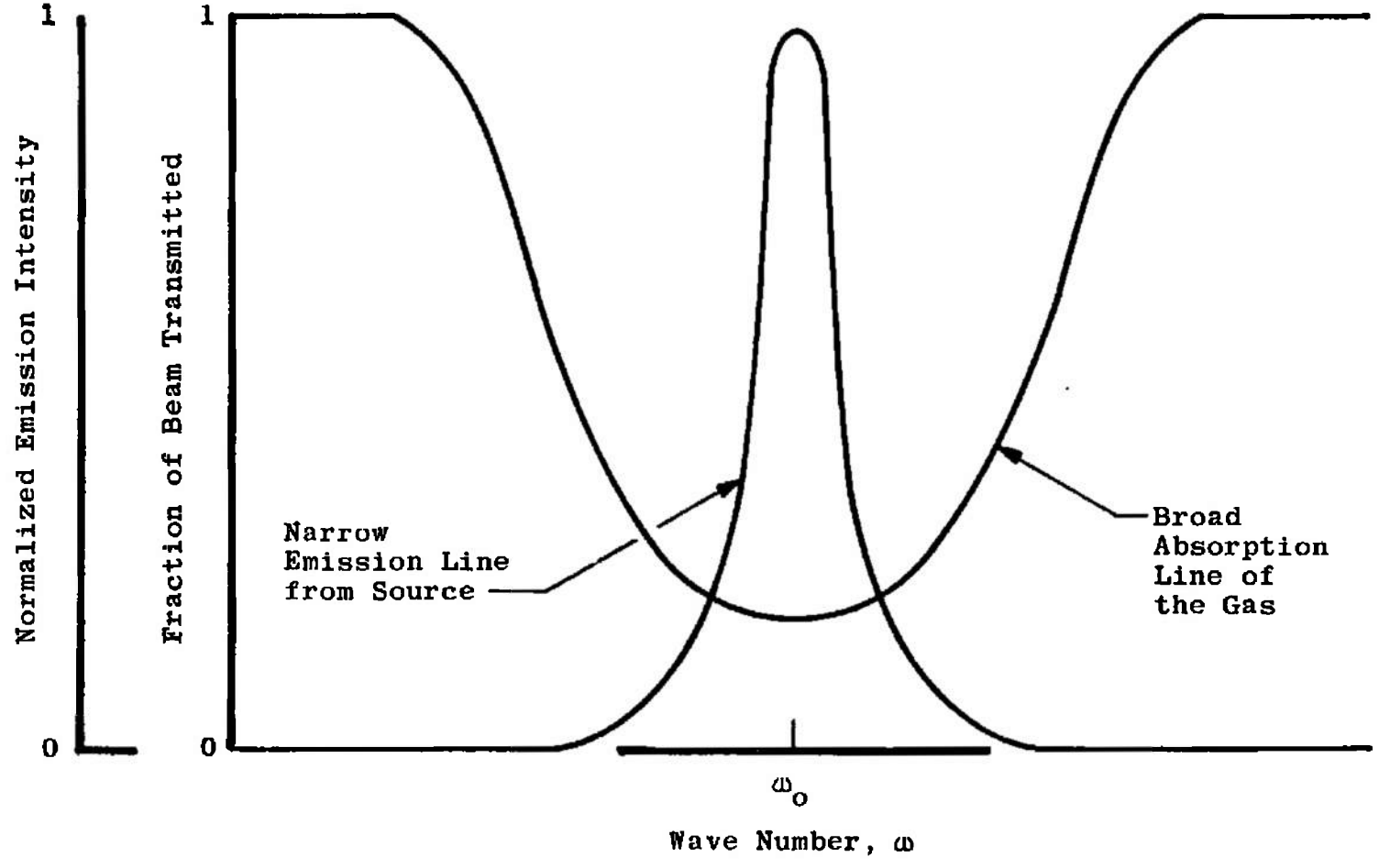


Fig. 9 Illustration Showing Principle of Spectral Line Absorption Technique

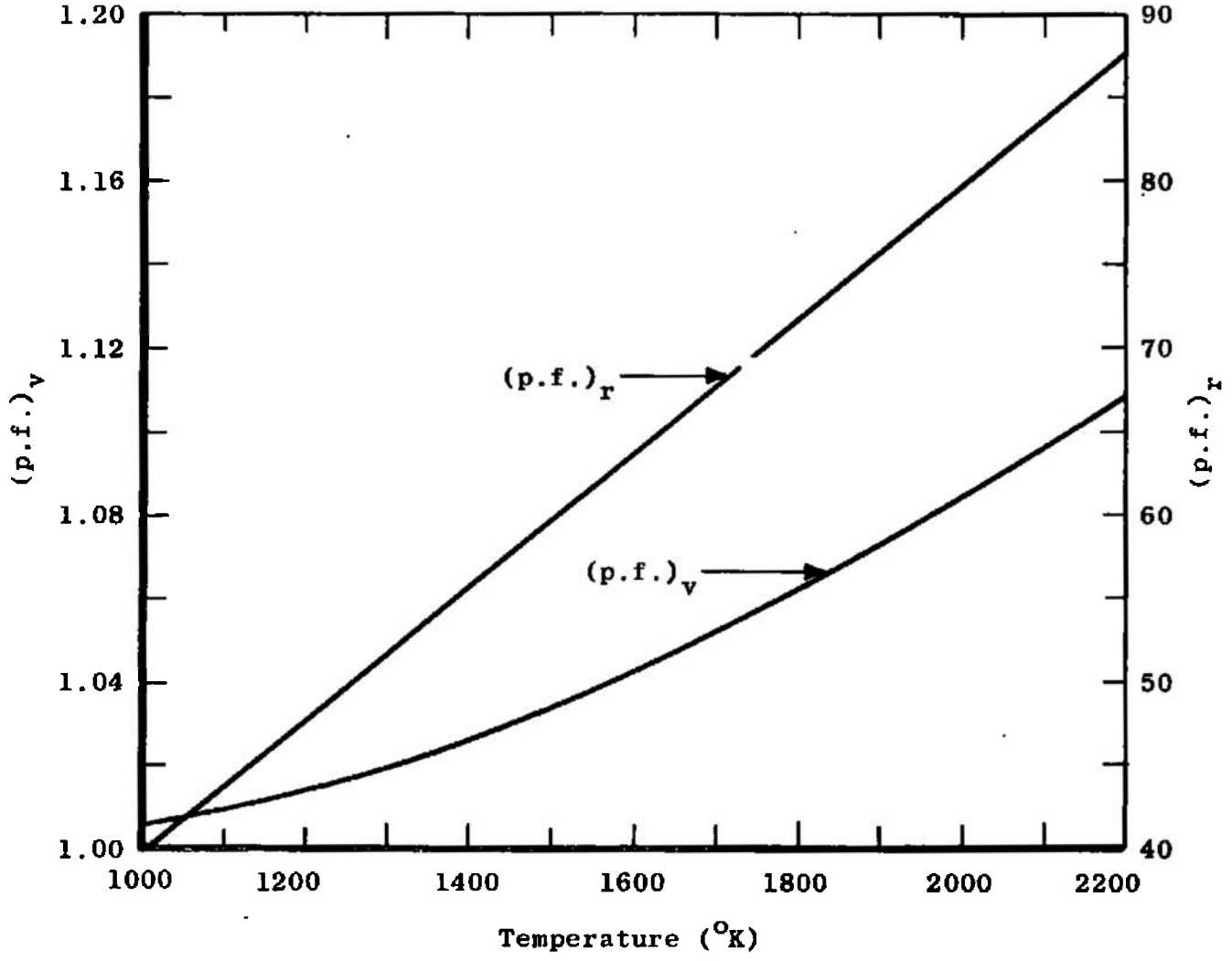


Fig. 10 Vibrational, $(p.f.)_v$, and Rotational, $(p.f.)_r$, Partition Functions of the Ground, $^2\Pi$, State of the OH Radical as a Function of Temperature

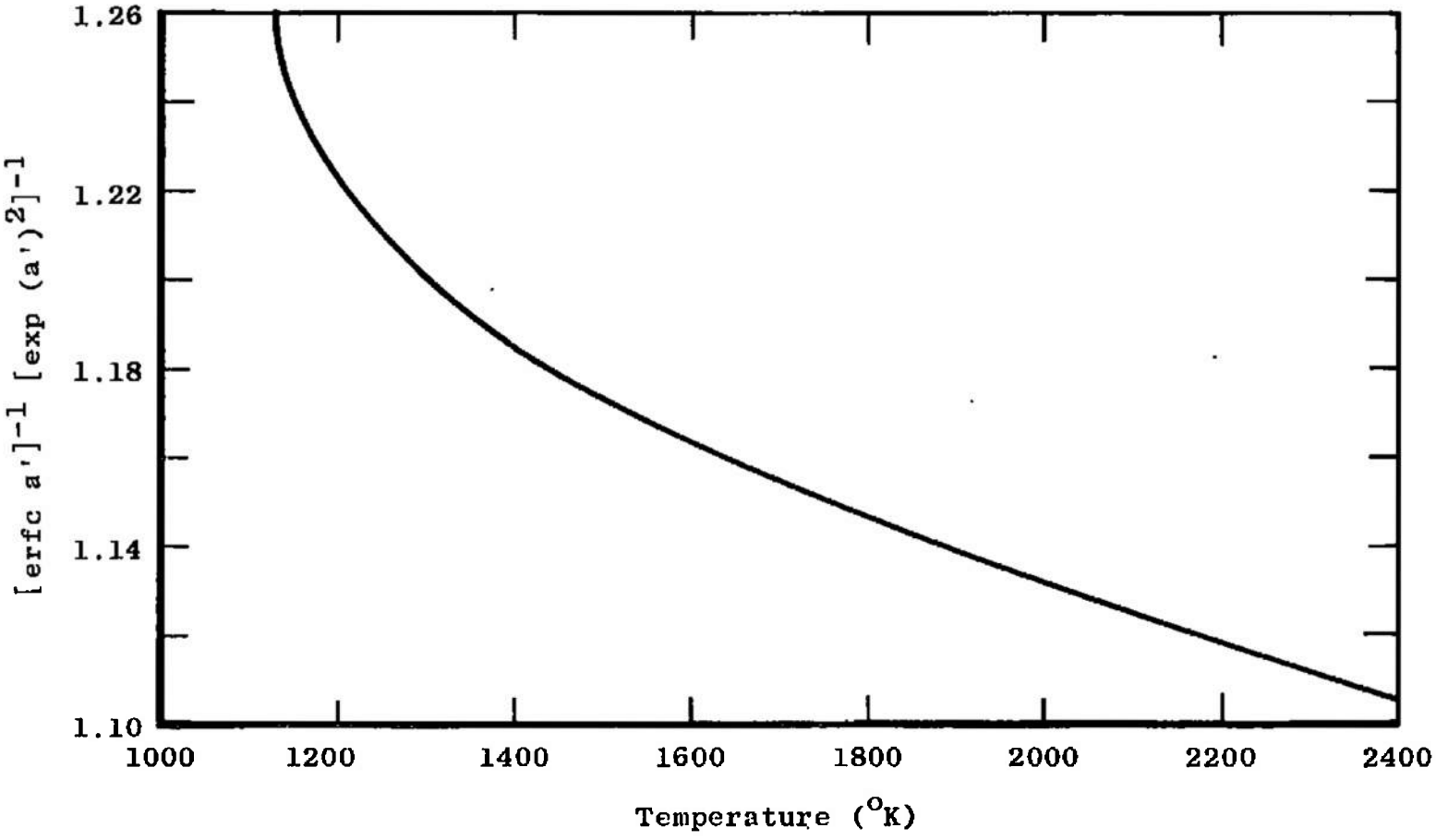


Fig. 11 Broadening Factor for OH Spectral Lines as a Function of Temperature for a Fixed Pressure of One-Half Atmosphere

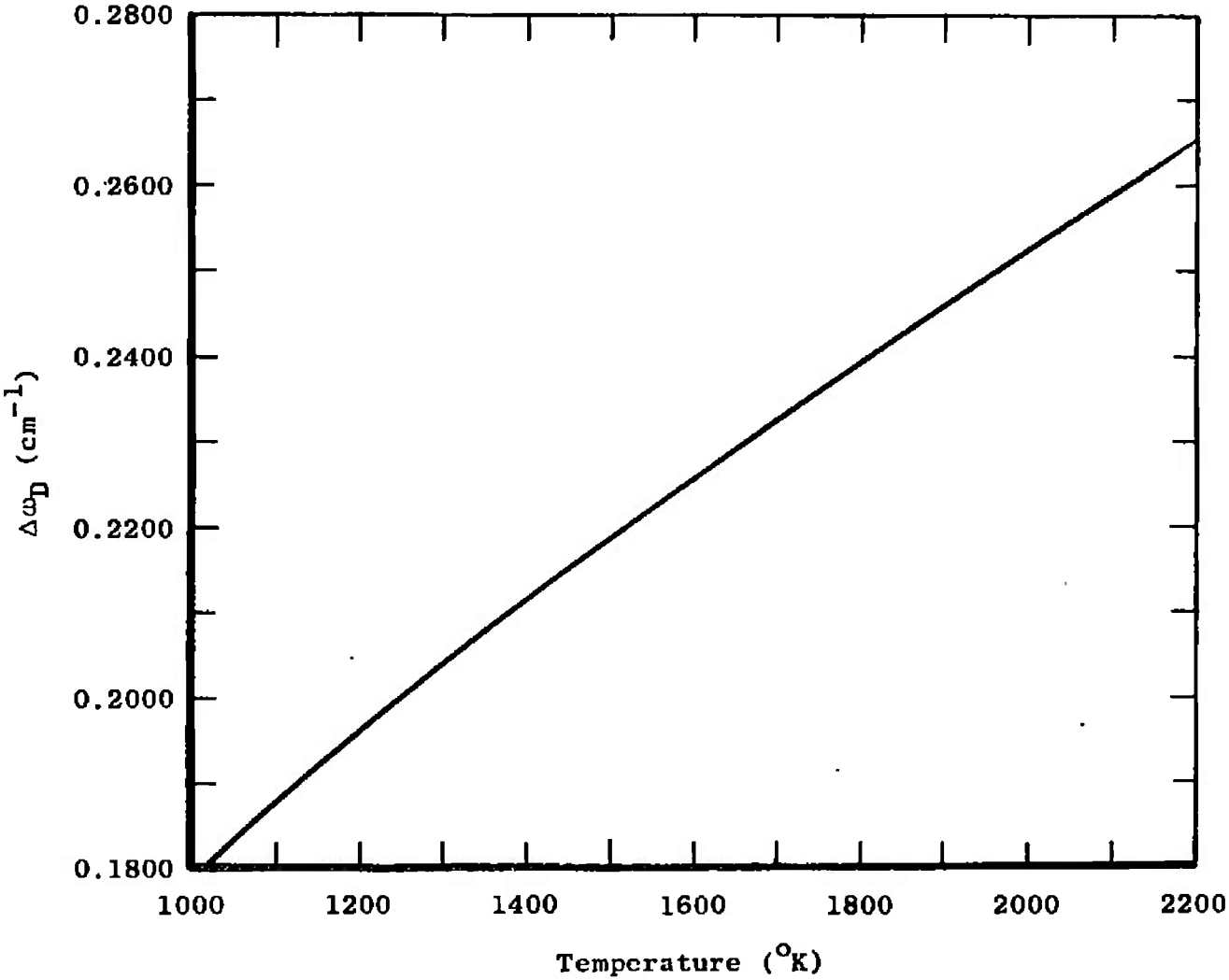


Fig. 12 Doppler Width, $A\omega_D$, of the $R_2^3$ Spectral Line of the $A\ ^2\Sigma+ - X\ ^2\Pi_i$ (0,0) Band of OH at Half Intensity as a Function of Temperature

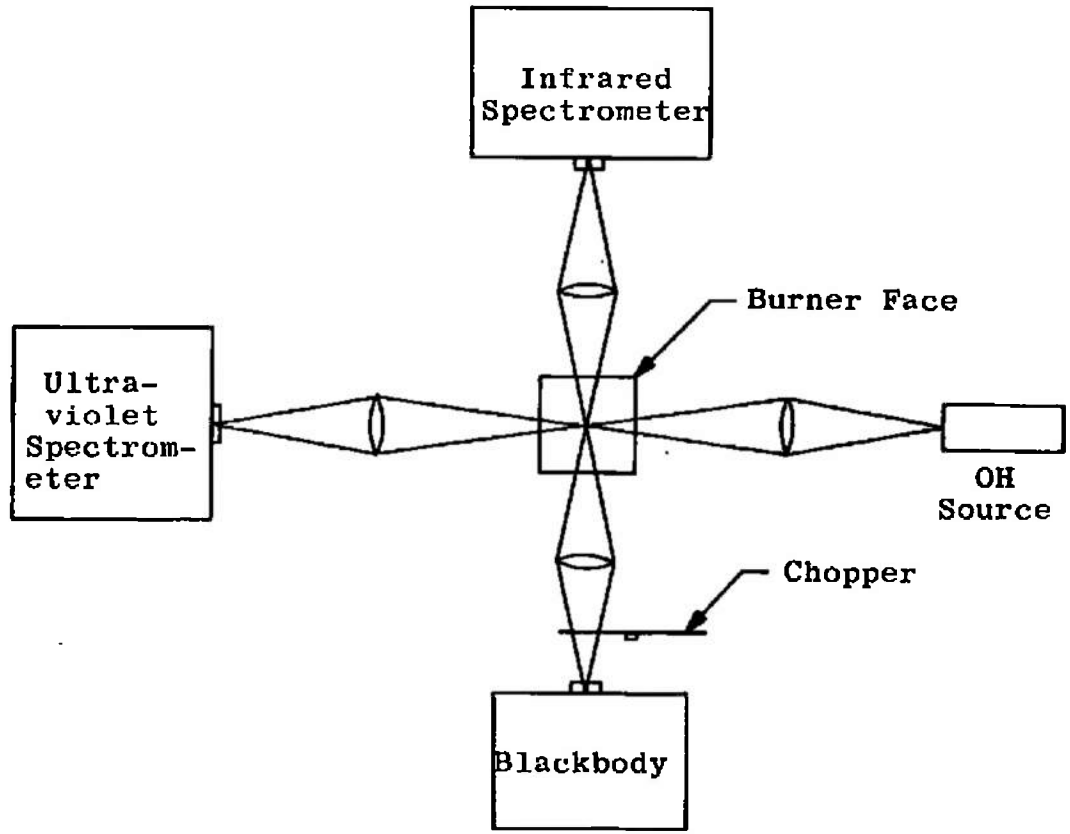


Fig. 13 Optical Arrangement of Spectrometers about the Burner

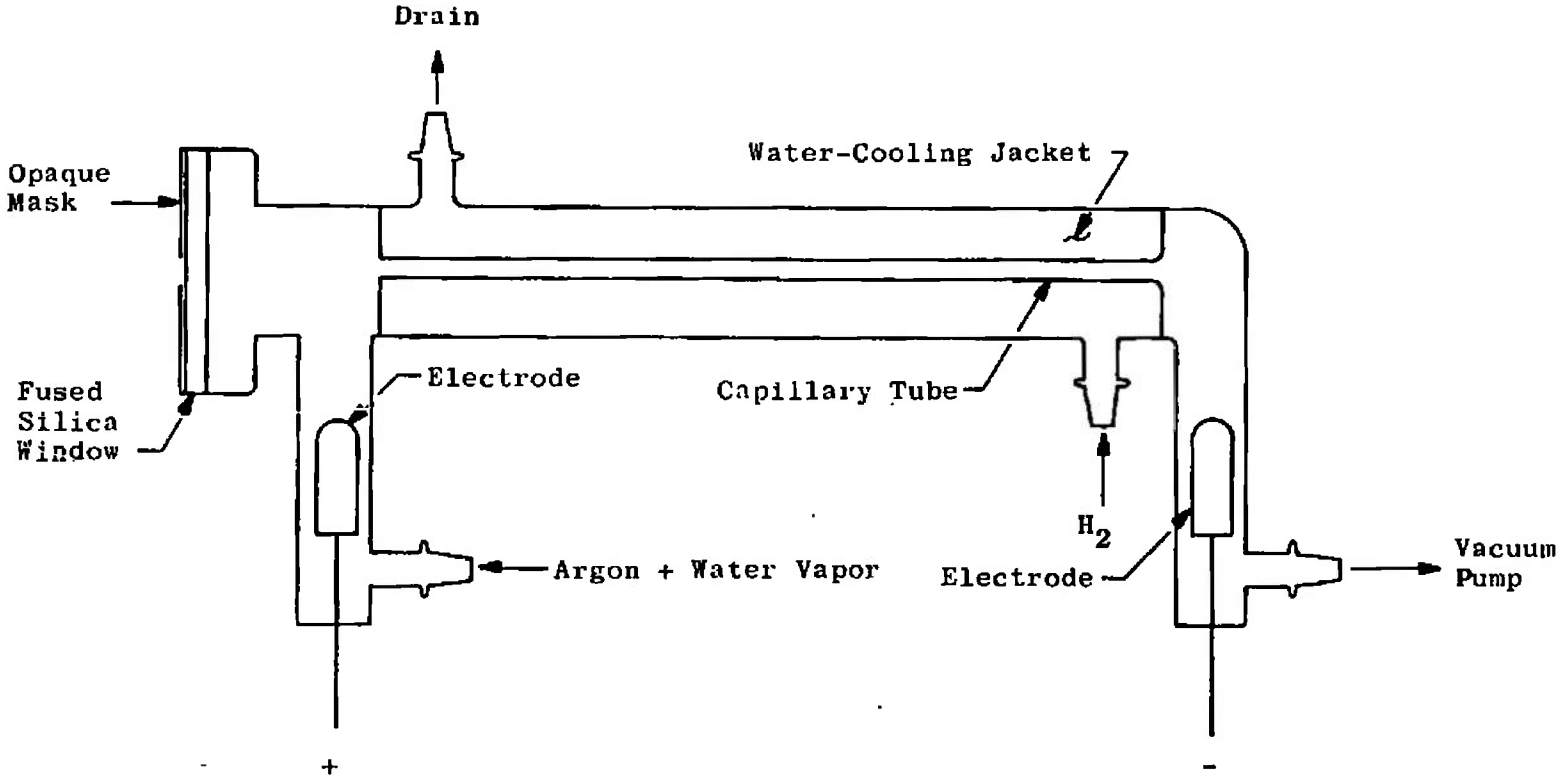


Fig. 14 Water Vapor Discharge Tube Used to Give Narrow Line Emission of the OH Spectra

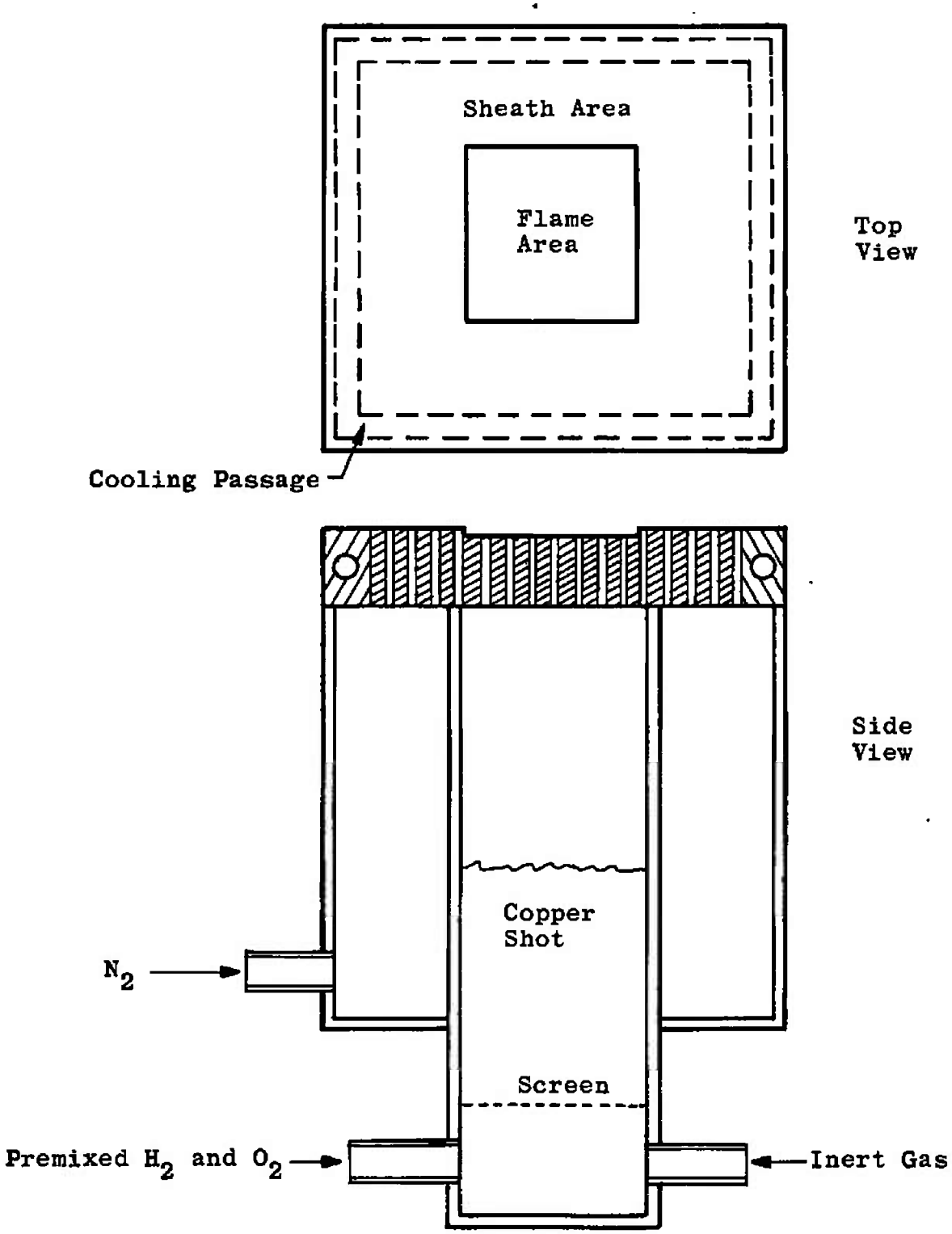


Fig. 15 Diagram of Flat Flame Burner Used in OH Chemiluminescent Studies

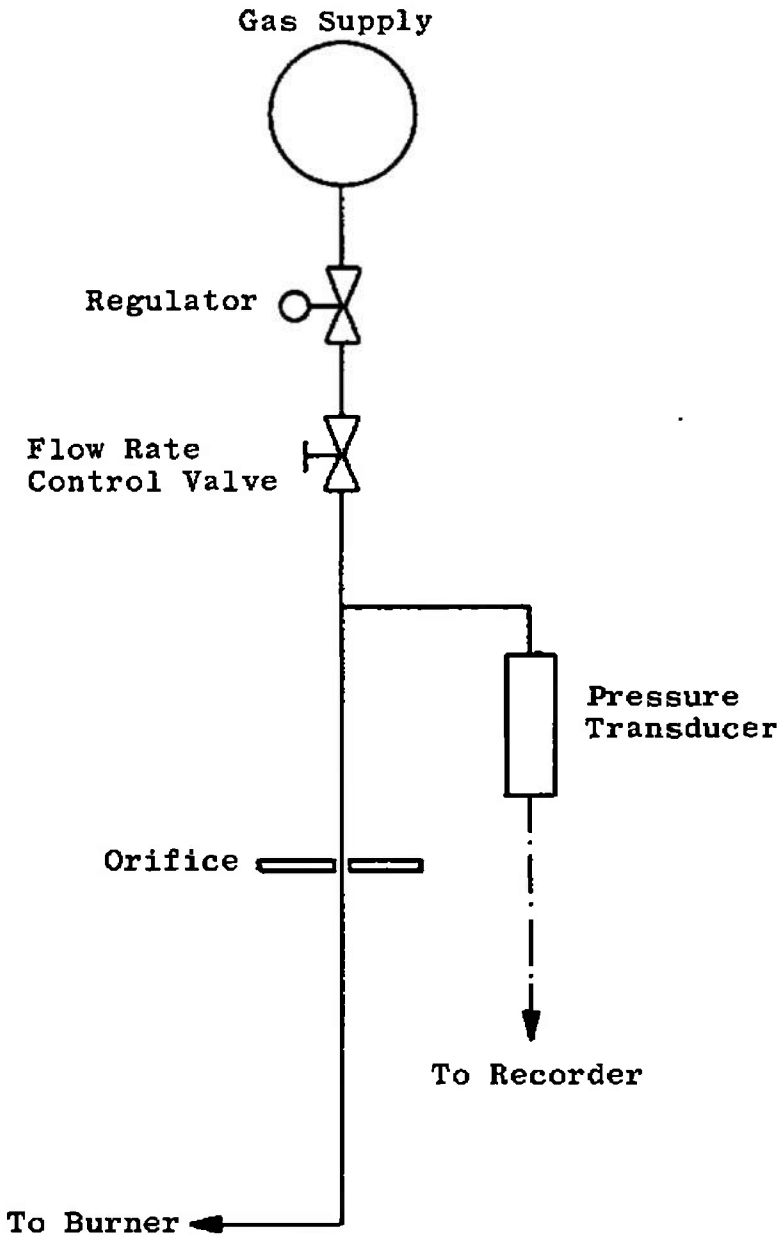


Fig. 16 Gas Control and Measuring System

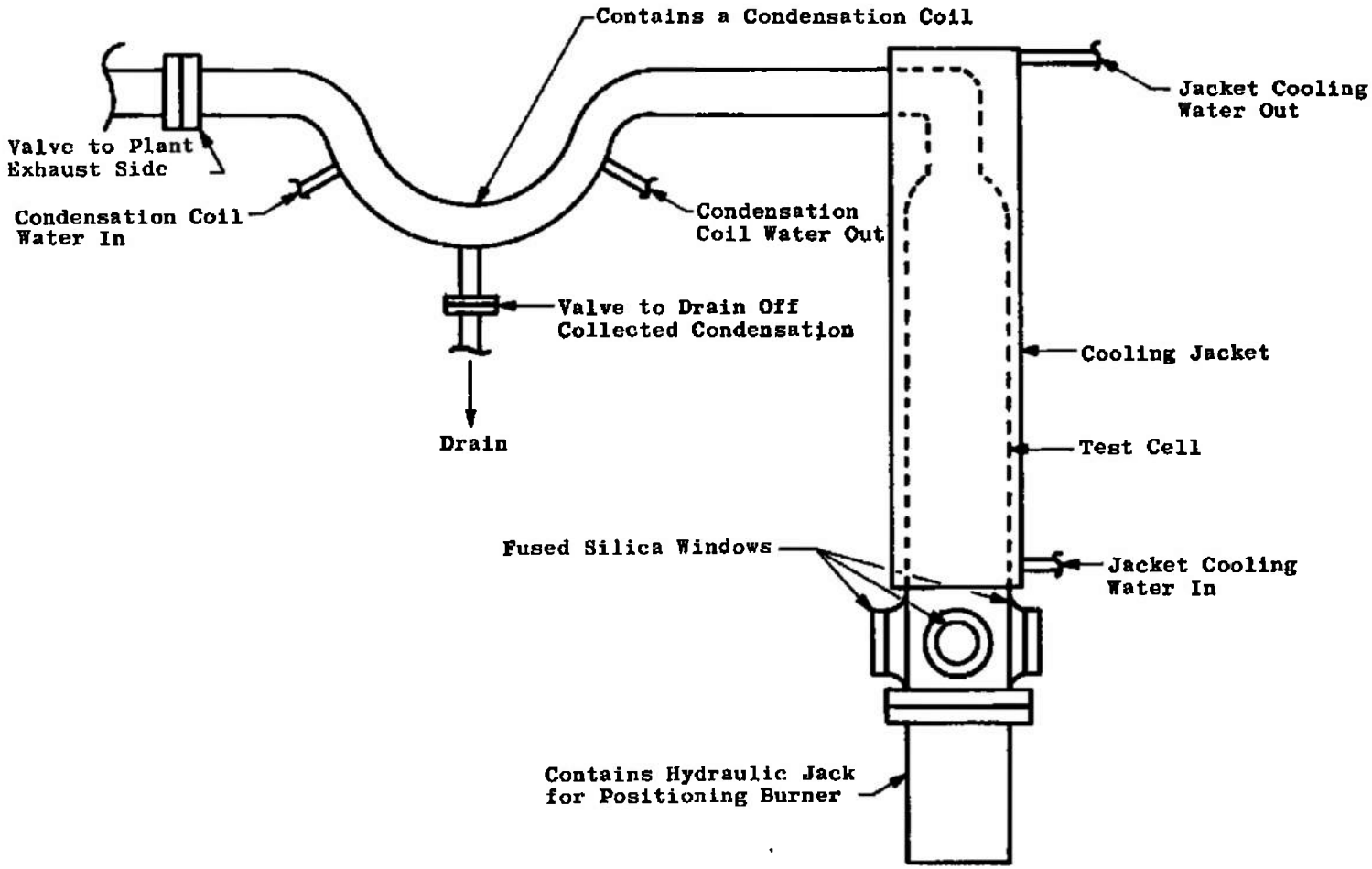


Fig. 17 Schematic of Test Cell

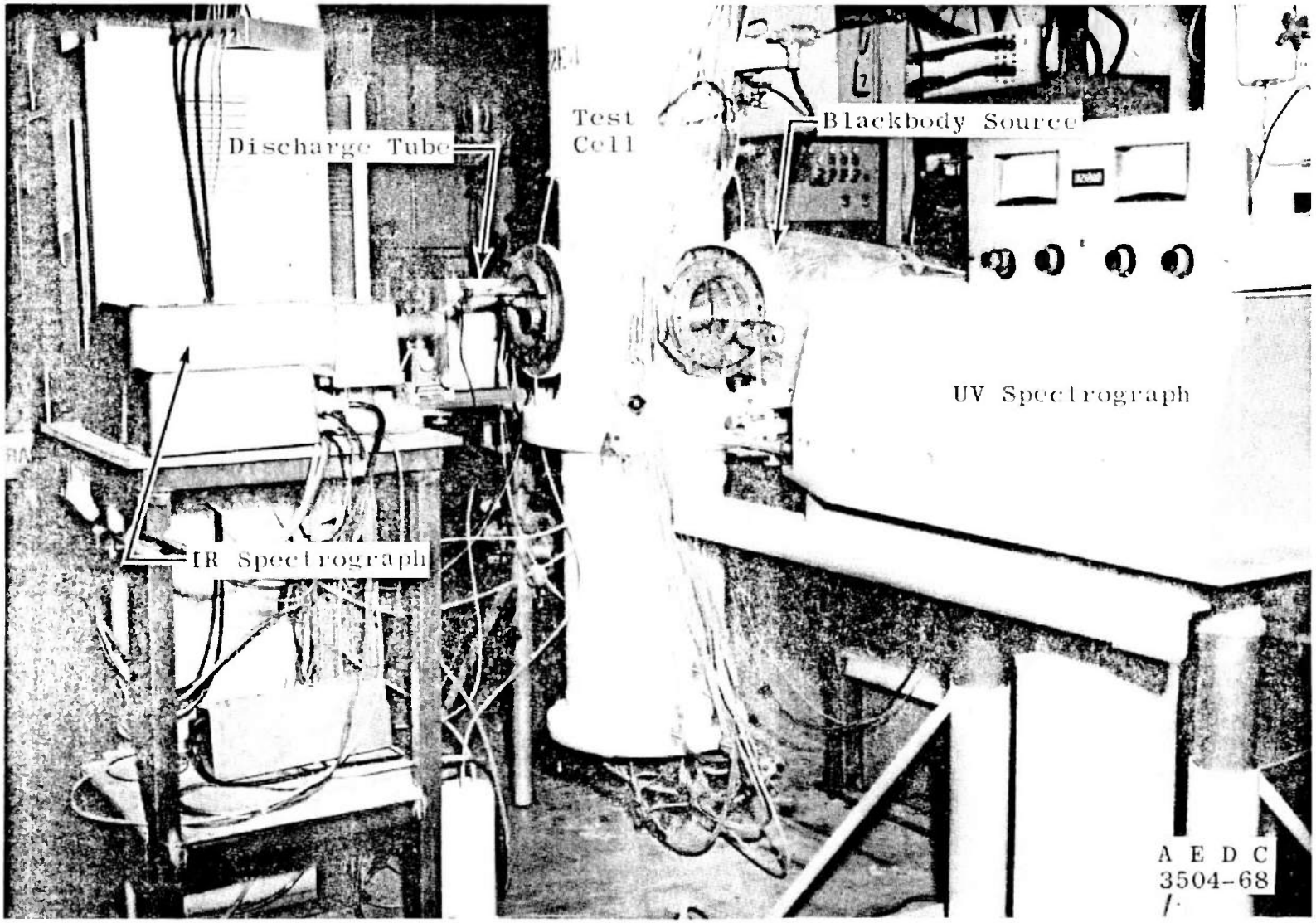


Fig. 18 Photograph Showing Arrangement of Equipment around the Test Cell

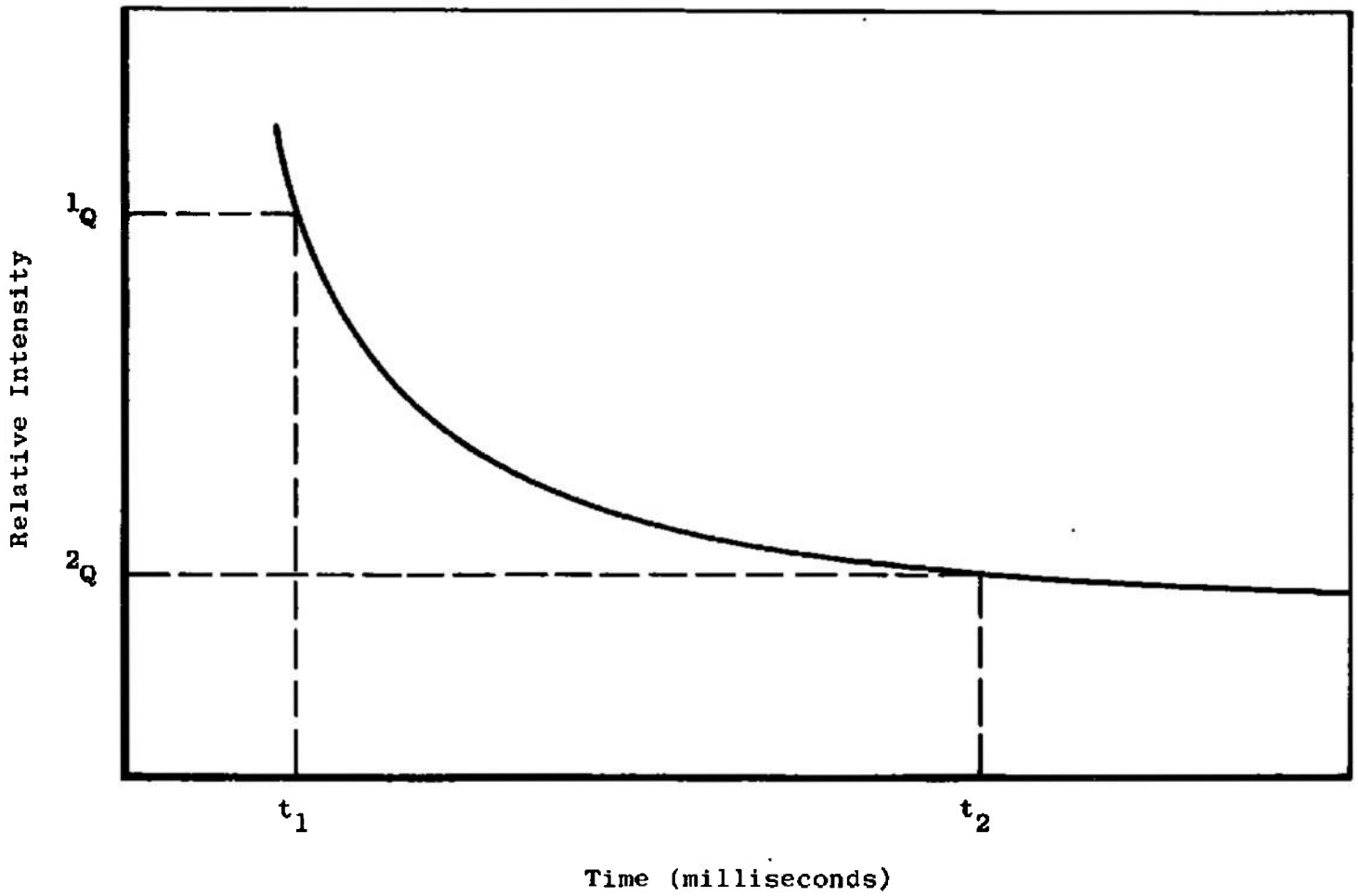


Fig. 19 Example of Relative Intensity of Radiation from A $^2\Sigma^+ \rightarrow X\ ^2\Pi_i$ (0,0) Transition of OH as a Function of Time Downstream of the Reaction Zone for a $H_2 - O_2$ Flame

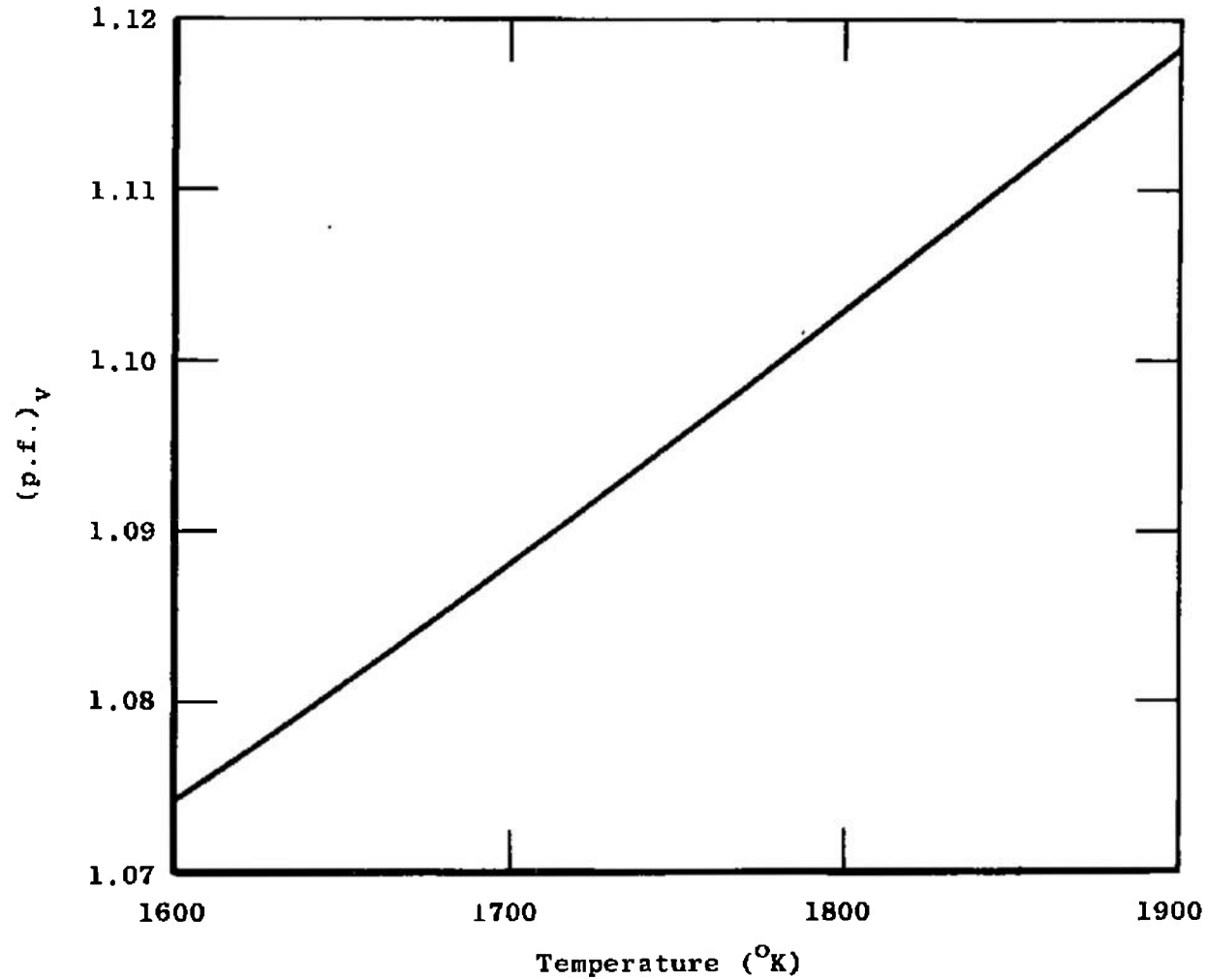


Fig. 20 Vibrational Partition Function for the $^{2}\Sigma^{+}$ Electronic State as a Function of Temperature for the OH Molecule

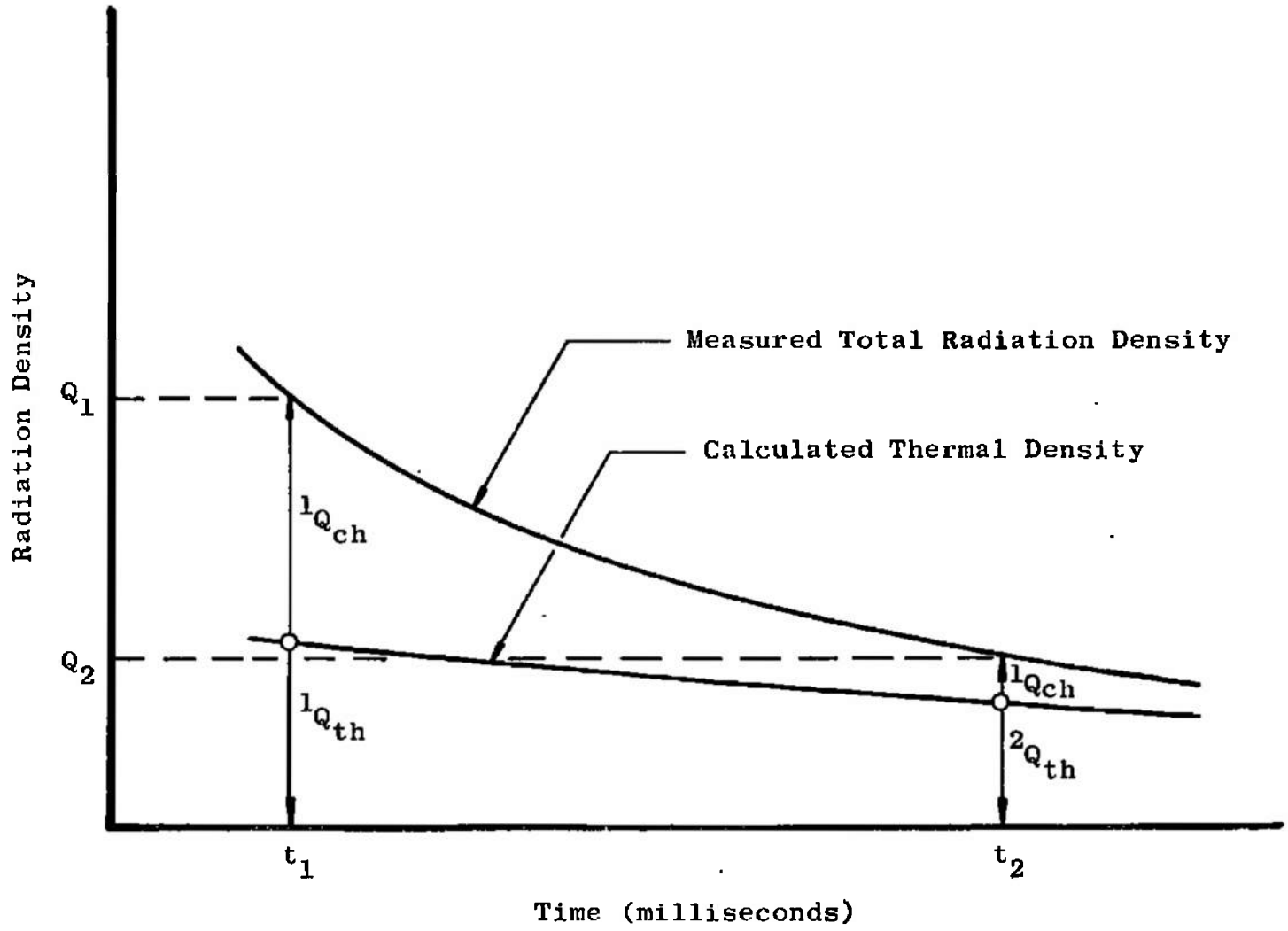


Fig. 21 Example Showing the Relation between the Total Radiation Density, the Thermal Radiation Density, and the Chemiluminescent Radiation Density

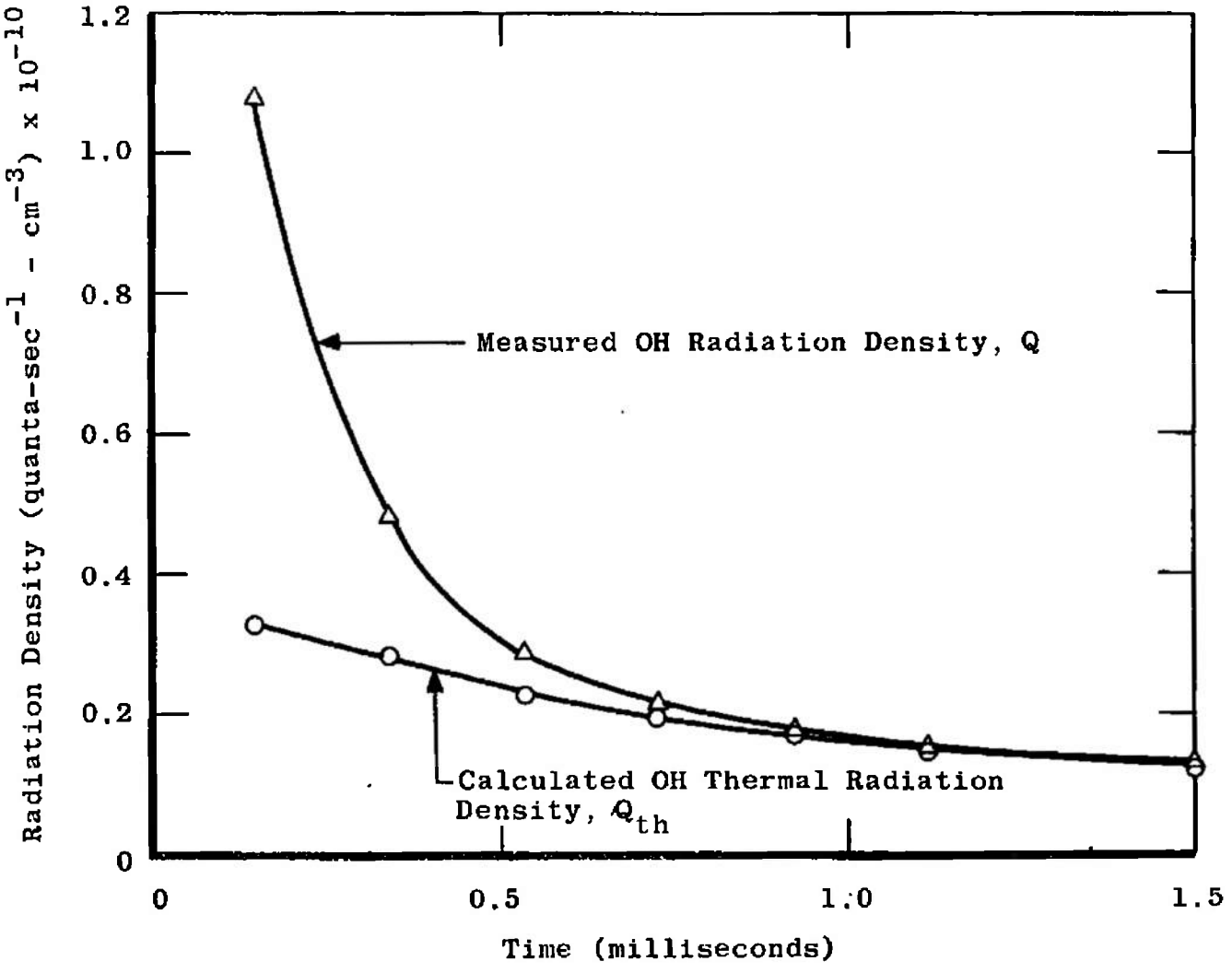


a. Flame 1

Fig. 22 Total and Thermal Radiation Density from A $^2\Sigma^+ \rightarrow X\ ^2\Pi_i$ (0,0) Transition of OH as Functions of Time Downstream of the Reaction Zone

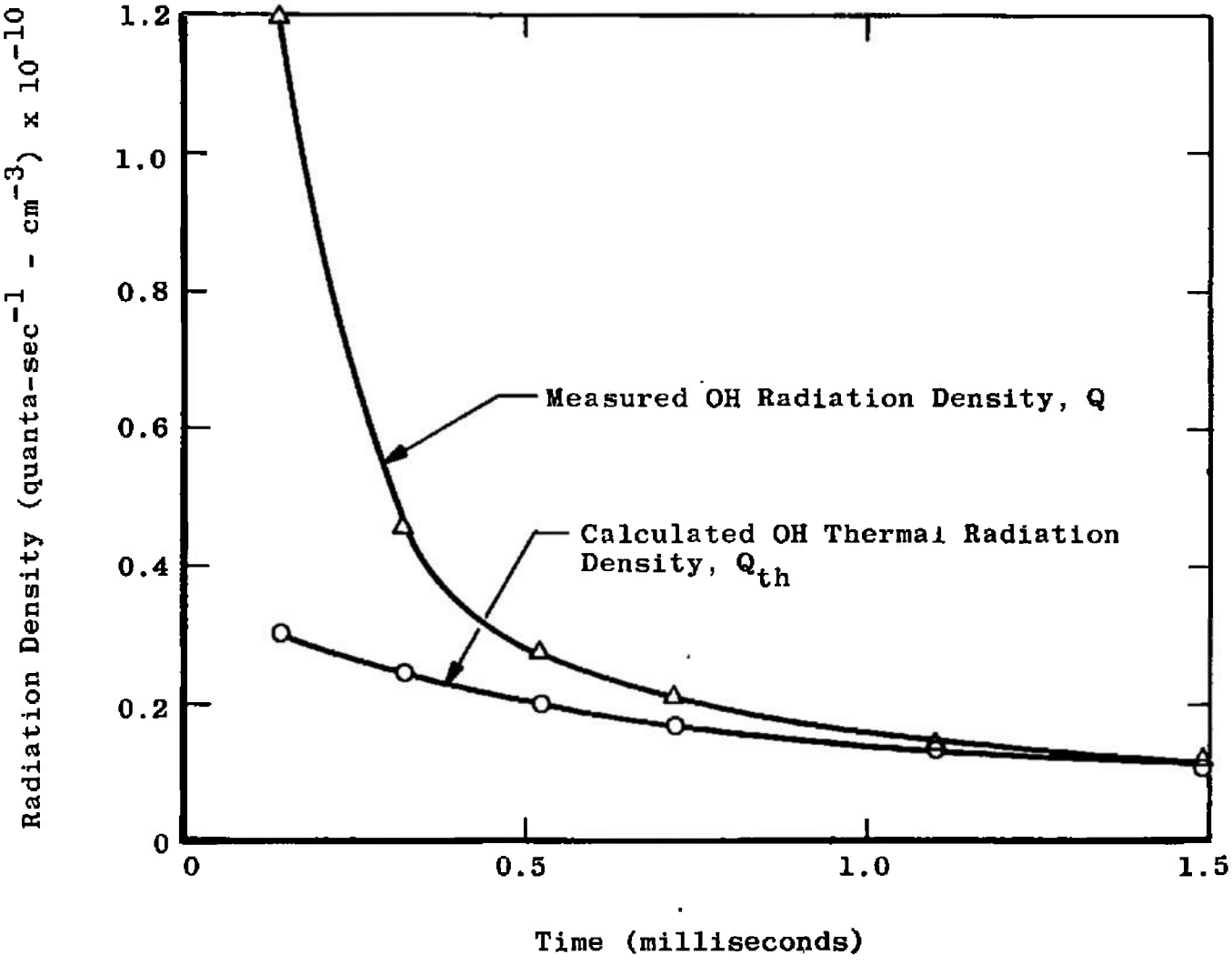


b. Flame 2

Fig. 22 Continued

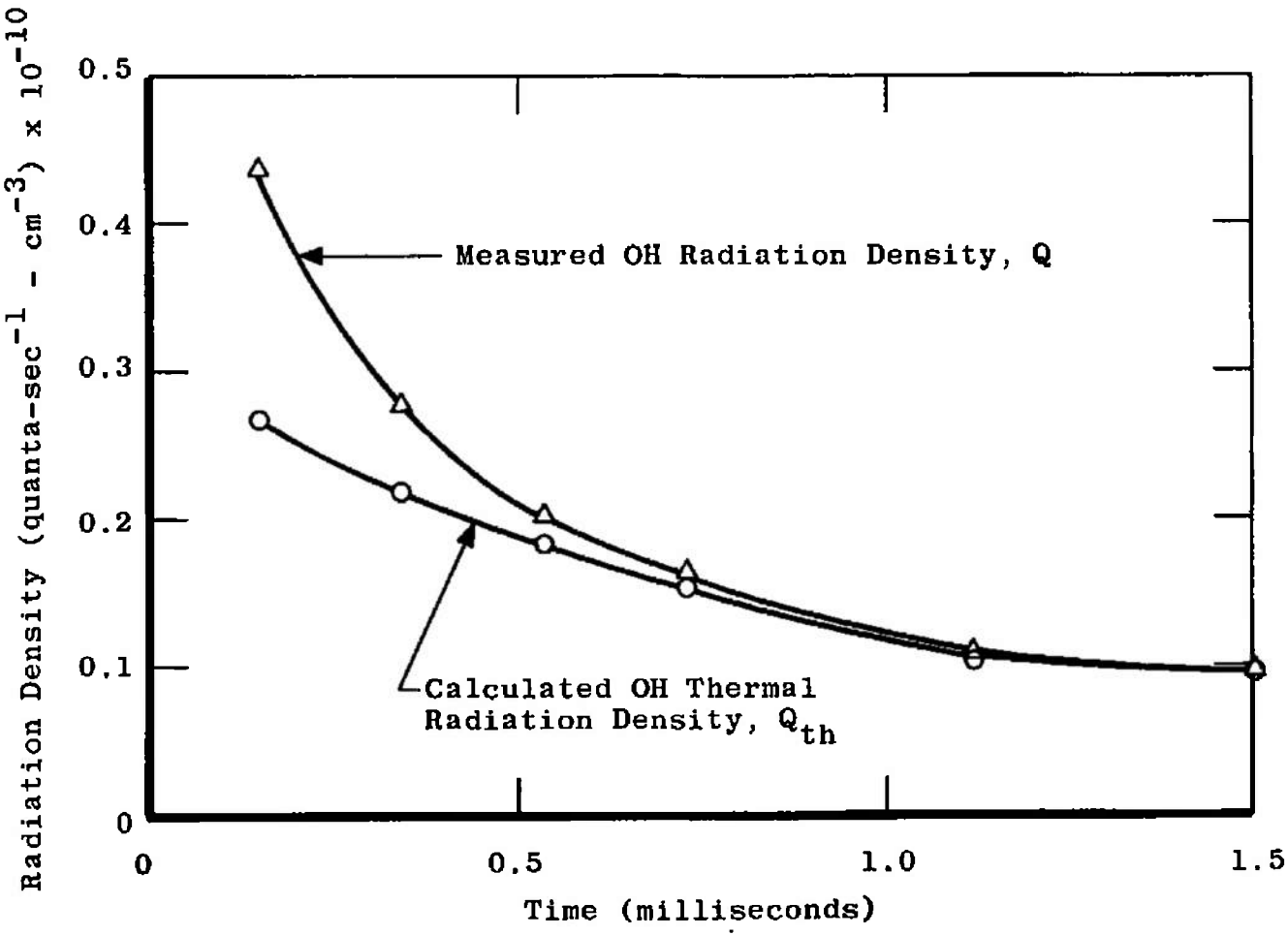


c. Flame 3

Fig. 22 Continued

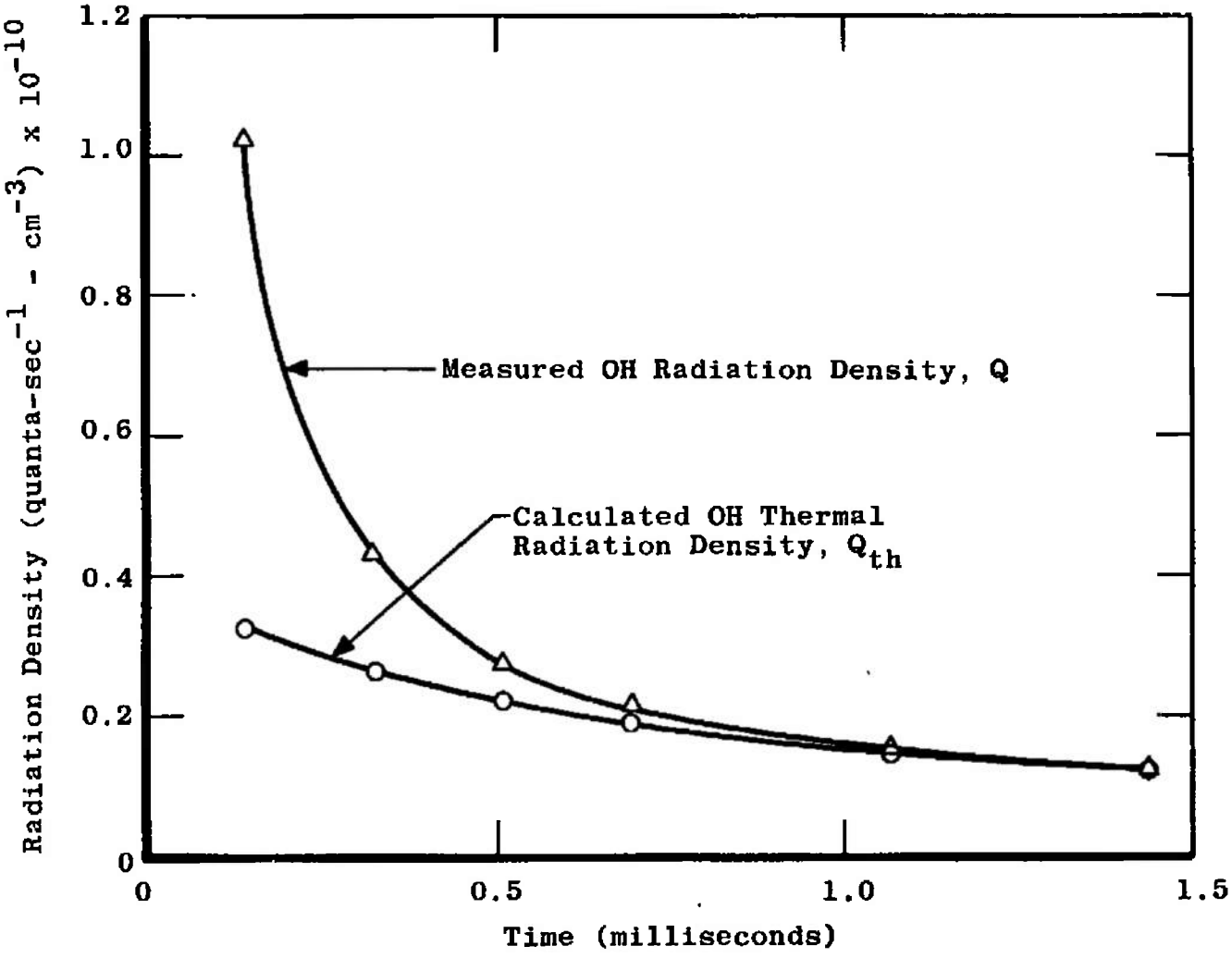


d. Flame 4

Fig. 22 Continued

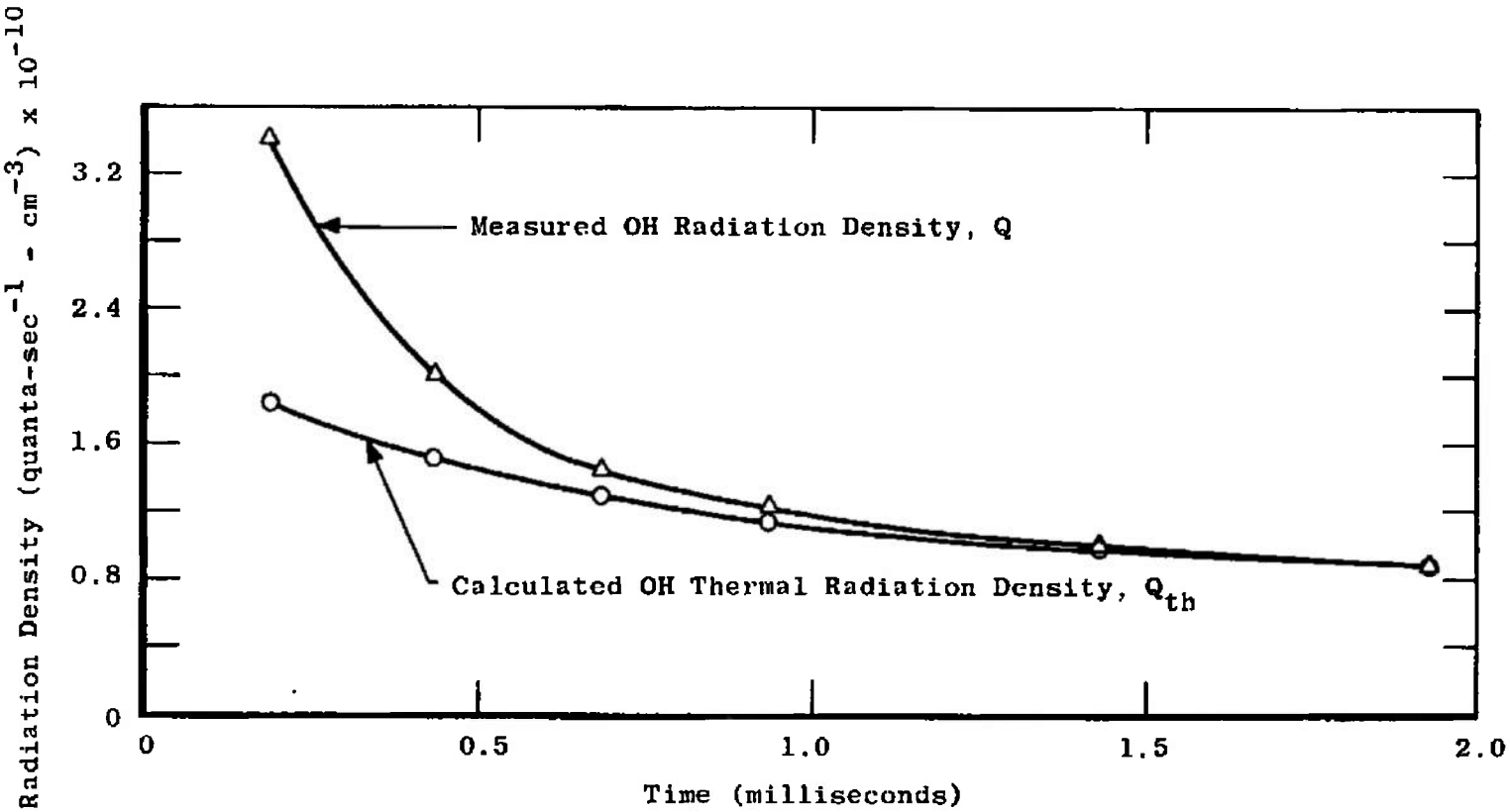


c. Flame 5

Fig. 22 Continued

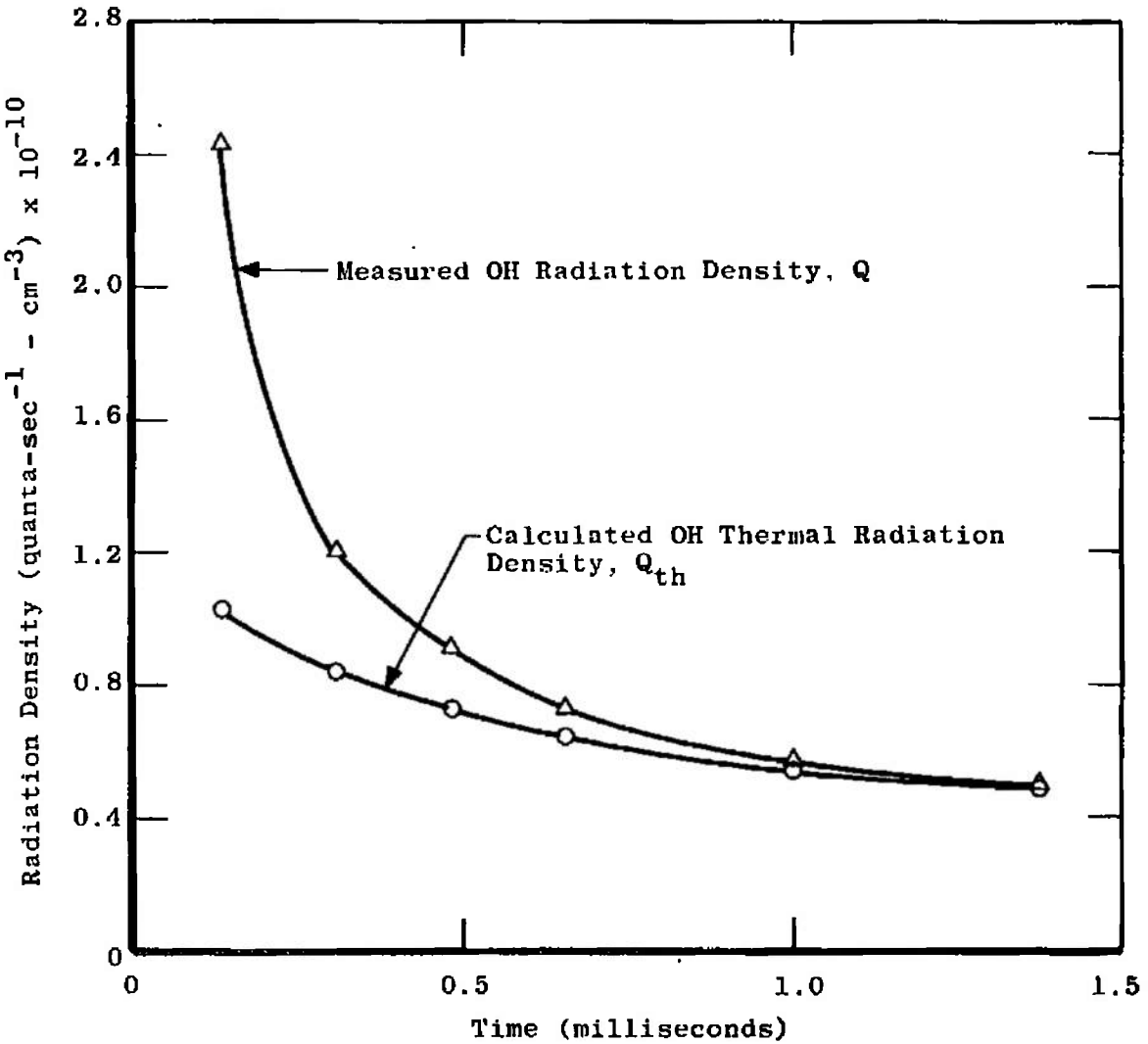


f. Flame 6

Fig. 22 Concluded

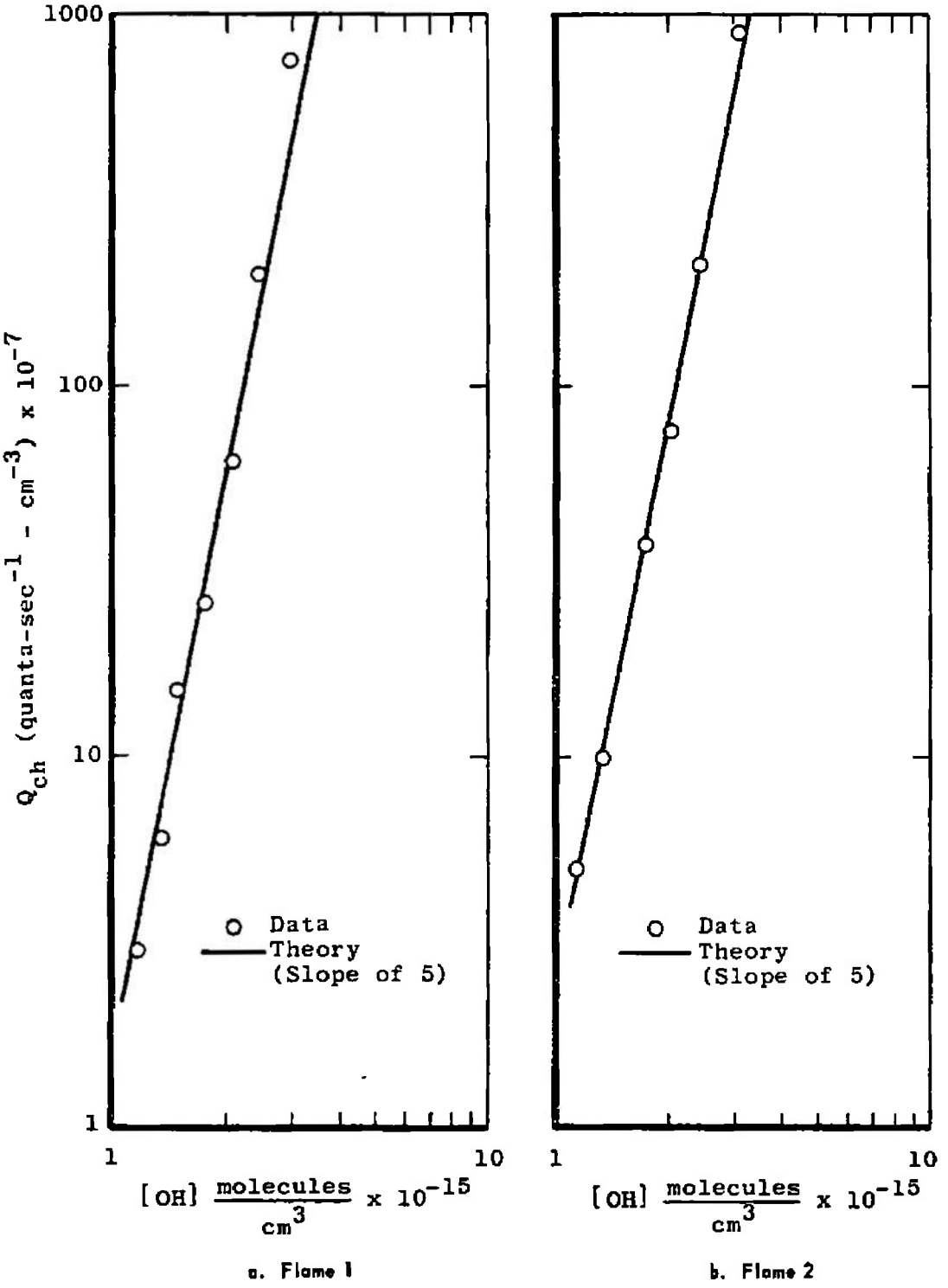


Fig. 23 Chemiluminescent Radiation Density from A $^2\Sigma^+ \rightarrow X\ ^2\Pi_i$ (0,0) Transitions of OH as a Function of OH Concentration

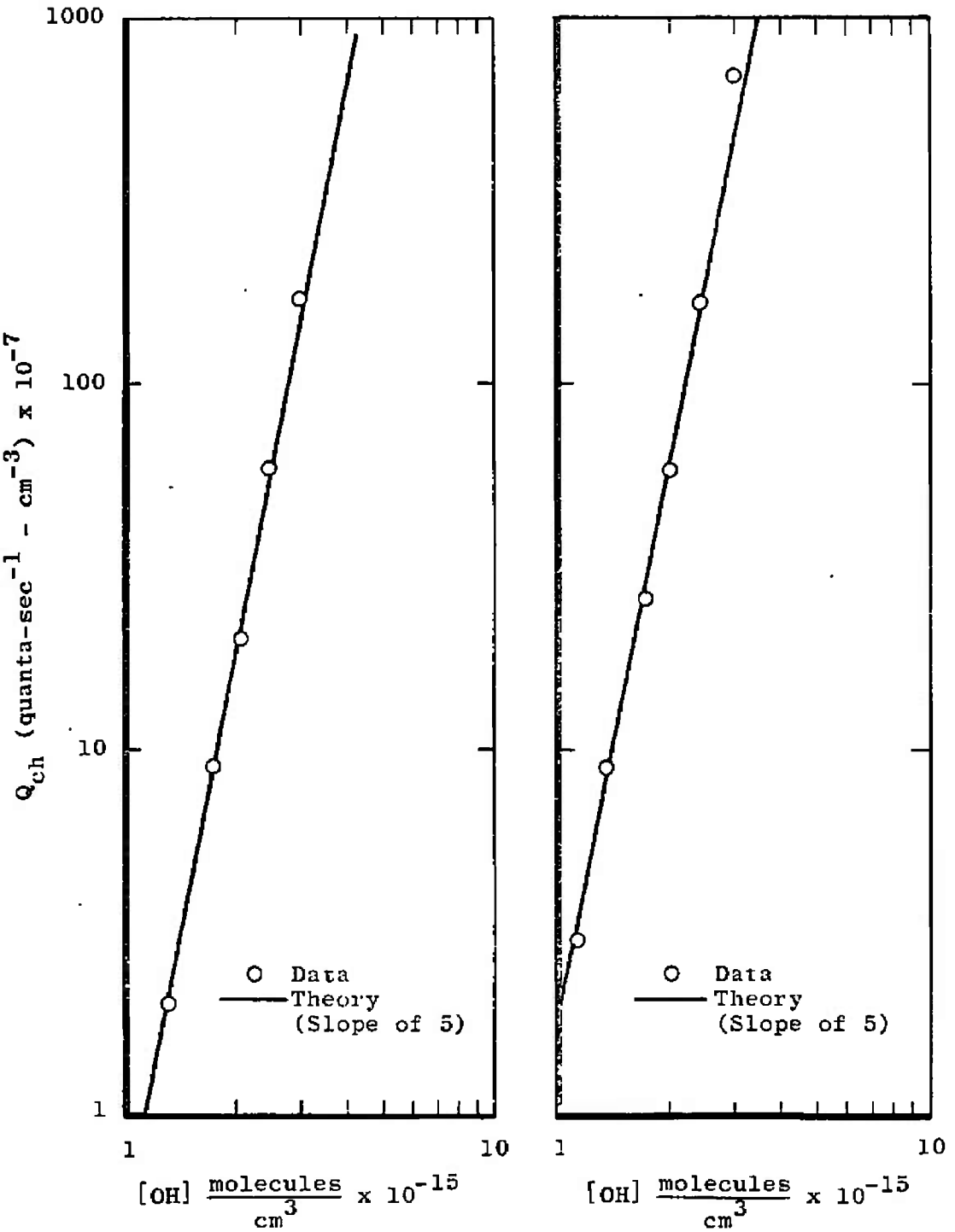


c. Flame 3

d. Flame 4

Fig. 23 Continued

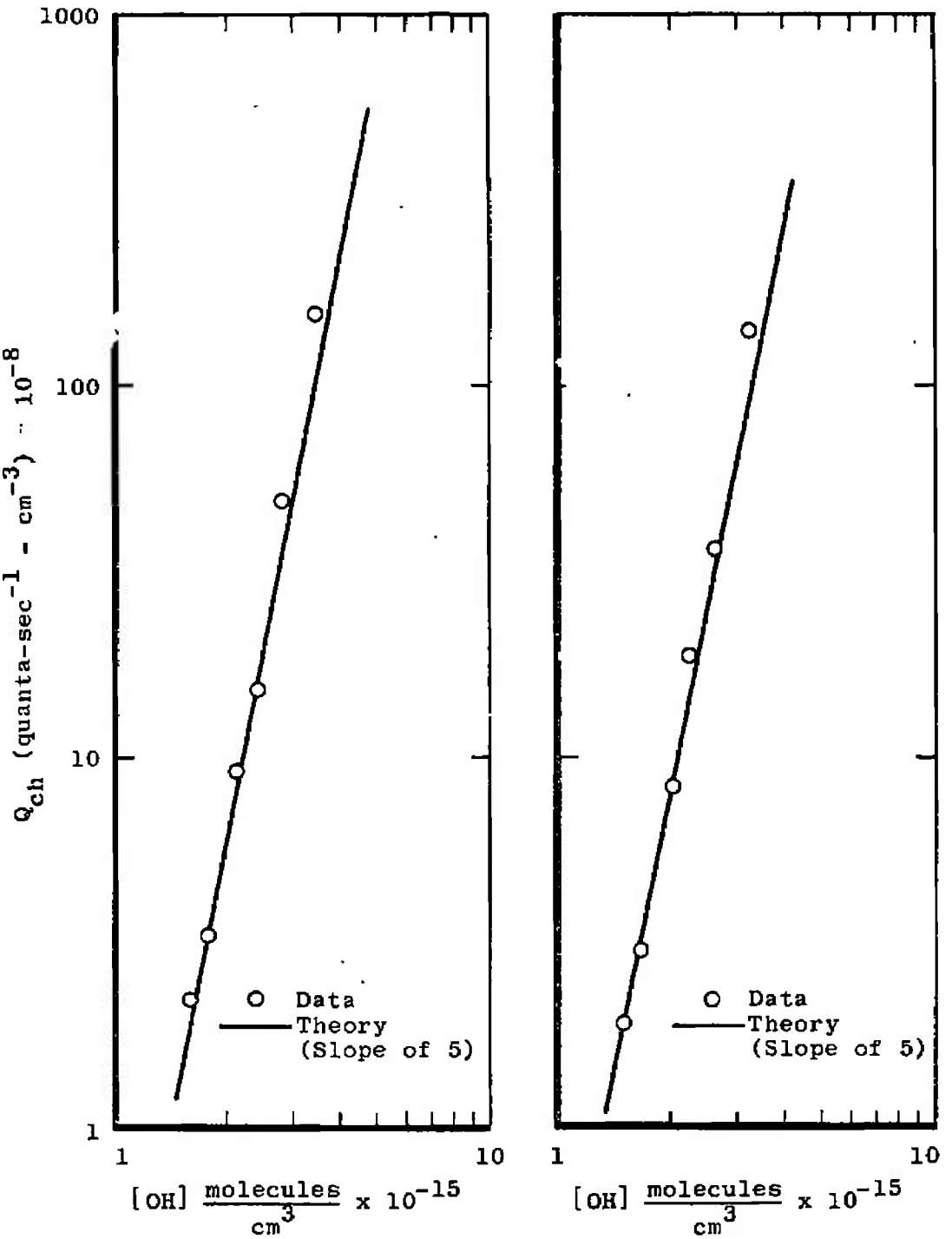


e. Flame 5

f. Flame 6

Fig. 23 Concluded

**TABLE I**
**ENERGY EXCESS AFTER EXCITATION OF OH FOR SPECIFIED CHEMICAL REACTIONS***

| Reactants | ΔE, ev, for $OH^2\Sigma$ in v' = | | | |
|---|---|---|---|---|
| | 0 | 1 | 2 | 3 |
| H + OH + OH | 1.19 | 0.82 | 0.48 | 0.16 |
| O + H + M | 0.37 | 0 | -0.33 | -0.66 |
| $O + H_2 + OH$ | 1.04 | 0.67 | 0.33 | 0 |
| $H + H_2 + O_2$ | 0.35 | -0.01 | 0.35 | -0.68 |

*Taken from Ref. 7.

**TABLE II**
**FLAME CHARACTERISTICS**

| Flame No. | Premixed Gas Volume Ratios | | | OH x $10^{-16}$ molecules-$cm^{-3}$ Maximum | OH x $10^{-16}$ molecules-$cm^{-3}$ Minimum | Temperature, °K |
|---|---|---|---|---|---|---|
| | $\frac{H_2}{O_2}$ | $\frac{H_2}{D}$ | D | | | |
| 1 | 1.000 | 0.385 | $N_2$ | 0.296 | 0.116 | 1750 |
| 2 | 0.900 | 0.400 | $N_2$ | 0.306 | 0.114 | 1745 |
| 3 | 0.800 | 0.417 | $N_2$ | 0.298 | 0.106 | 1740 |
| 4 | 0.700 | 0.445 | $N_2$ | 0.298 | 0.112 | 1750 |
| 5 | 0.700 | 0.375 | Ar | 0.343 | 0.160 | 1860 |
| 6 | 0.700 | 0.375 | He | 0.323 | 0.150 | 1830 |

## TABLE III
## SPECIES CONCENTRATION FOR FLAMES LISTED IN TABLE II

| Flame No. | Time, msec | $[OH] \times 10^{-15}$, molecules-cm$^{-3}$ | $[H_2O] \times 10^{-17}$, molecules-cm$^{-3}$ | $[O_2] \times 10^{-17}$, molecules-cm$^{-3}$ | $[H] \times 10^{-13}$, molecules-cm$^{-3}$ | $[D] \times 10^{-18}$, molecules-cm$^{-3}$ |
|---|---|---|---|---|---|---|
| 1 | 0.15 | 2.96 | 5.10 | 2.55 | 1.87 | 1.33 |
| | 0.34 | 2.46 | 5.10 | 2.55 | 1.07 | 1.33 |
| | 0.54 | 2.07 | 5.10 | 2.55 | 0.64 | 1.33 |
| | 0.73 | 1.74 | 5.10 | 2.56 | 0.38 | 1.33 |
| | 0.92 | 1.48 | 5.11 | 2.56 | 0.24 | 1.33 |
| | 1.12 | 1.34 | 5.11 | 2.56 | 0.17 | 1.33 |
| | 1.31 | 1.23 | 5.11 | 2.56 | 0.11 | 1.33 |
| 2 | 0.14 | 3.06 | 5.10 | 3.11 | 1.74 | 1.28 |
| | 0.34 | 2.45 | 5.10 | 3.11 | 0.89 | 1.28 |
| | 0.53 | 2.03 | 5.11 | 3.11 | 0.50 | 1.28 |
| | 0.72 | 1.73 | 5.11 | 3.11 | 0.31 | 1.28 |
| | 0.92 | 1.51 | 5.11 | 3.11 | 0.20 | 1.28 |
| | 1.11 | 1.34 | 5.11 | 3.12 | 1.15 | 1.28 |
| | 1.30 | 1.22 | 5.11 | 3.12 | 0.11 | 1.28 |
| | 1.49 | 1.14 | 5.11 | 3.12 | 0.09 | 1.28 |
| 3 | 0.15 | 2.98 | 5.07 | 3.79 | 1.36 | 1.22 |
| | 0.34 | 2.45 | 5.07 | 3.79 | 0.75 | 1.22 |
| | 0.54 | 2.05 | 5.07 | 3.80 | 0.44 | 1.22 |
| | 0.73 | 1.72 | 5.07 | 3.80 | 0.26 | 1.22 |
| | 0.92 | 1.47 | 5.08 | 3.80 | 0.16 | 1.22 |
| | 1.12 | 1.30 | 5.08 | 3.80 | 0.11 | 1.22 |
| | 1.31 | 1.15 | 5.08 | 3.80 | 0.08 | 1.22 |
| | 1.51 | 1.06 | 5.08 | 3.80 | 0.06 | 1.22 |
| 4 | 0.15 | 2.98 | 5.00 | 4.64 | 1.07 | 1.13 |
| | 0.34 | 2.40 | 5.01 | 4.64 | 0.57 | 1.13 |
| | 0.54 | 2.00 | 5.01 | 4.64 | 0.32 | 1.13 |
| | 0.73 | 1.71 | 5.01 | 4.65 | 0.20 | 1.13 |
| | 0.92 | 1.49 | 5.01 | 4.65 | 0.13 | 1.13 |
| | 1.12 | 1.33 | 5.01 | 4.65 | 0.09 | 1.13 |
| | 1.31 | 1.22 | 5.01 | 4.65 | 0.07 | 1.13 |
| | 1.51 | 1.12 | 5.01 | 4.65 | 0.05 | 1.13 |
| 5 | 0.19 | 3.43 | 4.28 | 3.96 | 1.28 | 1.45 |
| | 0.44 | 2.82 | 4.28 | 3.97 | 0.71 | 1.45 |
| | 0.68 | 2.40 | 4.28 | 3.97 | 0.44 | 1.45 |
| | 0.93 | 2.12 | 4.28 | 3.97 | 0.30 | 1.45 |
| | 1.18 | 1.93 | 4.28 | 3.97 | 0.23 | 1.45 |
| | 1.43 | 1.79 | 4.29 | 3.97 | 0.18 | 1.45 |
| | 1.68 | 1.68 | 4.29 | 3.97 | 0.15 | 1.45 |
| | 1.93 | 1.60 | 4.29 | 3.97 | 0.13 | 1.45 |
| 6 | 0.13 | 3.23 | 4.35 | 4.03 | 1.19 | 1.64 |
| | 0.31 | 2.63 | 4.35 | 4.03 | 0.64 | 1.64 |
| | 0.48 | 2.28 | 4.35 | 4.04 | 0.42 | 1.64 |
| | 0.66 | 2.01 | 4.36 | 4.04 | 0.29 | 1.64 |
| | 0.83 | 1.82 | 4.36 | 4.04 | 0.21 | 1.64 |
| | 1.00 | 1.68 | 4.36 | 4.04 | 0.17 | 1.64 |
| | 1.18 | 1.58 | 4.36 | 4.04 | 0.14 | 1.64 |
| | 1.35 | 1.50 | 4.36 | 4.04 | 0.12 | 1.64 |

TABLE IV
FLAME COMPOSITION, RESONANCE YIELD FACTOR OF OH FLOURESCENCE, p, AND QUENCHING RATE, $k_{-m}$, FOR FLAME SPECIES*

| Flame No. | Composition in Mole Fractions | | Flame Temperature, °K | $p \times 10^3$ | $k_{-m}$ ($cm^3$-molecule$^{-1}$-sec$^{-1}$) $\times 10^{-9}$ |
|---|---|---|---|---|---|
| 1 | $H_2O$ | 0.21 | 1790 | 1.3 | 0.834 |
| | $O_2$ | 0.155 | | | 0.223 |
| | $A_R$ | 0.63 | | | 0 |
| 2 | $H_2O$ | 0.225 | 1760 | 0.9 | 0.834 |
| | $N_2$ | 0.77 | | | 0.120 |
| 3 | $H_2O$ | 0.21 | 1500 | 0.75 | 0.834 |
| | $O_2$ | 0.155 | | | 0.223 |
| | $N_2$ | 0.63 | | | 0.120 |

*Taken from Ref. 23.

TABLE V

EFFECTIVE REACTION RATES, RESONANCE YIELD FACTORS, AND EXCITATION RATES FOR SIX HYDROGEN FLAMES

| Flame No. | $pK_{IX} \times 10^{35}$ $cm^6$-molecule$^{-2}$-sec$^{-1}$ | $p \times 10^3$ | $K_{IX} \times 10^{32}$ $cm^6$-molecule$^{-2}$-sec$^{-1}$ |
|---|---|---|---|
| 1 | 2.23 | 1.63 | 1.37 |
| 2 | 3.97 | 1.62 | 2.45 |
| 3 | 1.43 | 1.61 | 0.89 |
| 4 | 4.39 | 1.60 | 2.74 |
| 5 | 6.72 | 2.35 | 2.86 |
| 6 | 7.17 | 2.36 | 3.04 |

## APPENDIX III
## COMPUTER PROGRAM FOR CALCULATING SPECIES CONCENTRATIONS IN LEAN $H_2$-$O_2$-D FLAMES

This program calculates species concentrations in lean $H_2$-$O_2$-D flames for temperatures less than 2500°K from measurements of the temperature and OH concentrations. It begins by solving the equation,

$$C^3[(2R+1)f'_{H_2O} + f'_{O_2}] - C^2[n - (R+1)[OH]]$$

$$+ C\left[(2R+1)K_{H_2}\frac{[OH]^2}{f'_{O_2}} - K_O\frac{[OH]^2}{f'_{H_2O}}\right]$$

$$+ (R+1)K_H\frac{[OH]^3}{f'_{H_2O}f'_{O_2}} = 0$$

for C, where

$$R = \frac{\text{Volume Flow Rate of D}}{2 \times \text{Volume Flow Rate of } H_2}$$

n is the number density of molecules, which is a function of T, and the f′'s are equilibrium mole fractions as found in $H_2$-$O_2$ equilibrium tables (Ref. 24) and are functions of T and equivalence ratios.

The species concentrations are then calculated from the equations:

$$[H_2O] = C f'_{H_2O}$$

$$[O_2] = C f'_{O_2}$$

$$[H] = K_H\frac{[OH]^3}{C^2 f'_{H_2O} f'_{O_2}}$$

$$[H_2] = K_{H_2}\frac{[OH]^2}{C f'_{O_2}}$$

$$[O] = K_O\frac{[OH]^2}{C f'_{H_2O}}$$

## I. MAIN PROGRAM

```
      IMPLICIT REAL*8(A-H,O-Z)
      COMPLEX*8 R1,R2,R3,R4
      DIMENSION OHI(50),NP(50)
   10 READ (5,90)NPOS,NFLAM
      IF (NPOS.EQ.0) GO TO 50
      WRITE (6,140) NFLAM
      READ (5,110) R,PH20,PO2,XKH2,XKO,XKH,T,SCAL
      READ (5,110) (OHI(K),K=1,NPOS)
      READ (5,90) (NP(K),K=1,NPOS)
      DO 40 I=1,NPOS
      OH=OHI(I)
      XN=3 67D+21/T
      T1=2 *R+1
      T2=R+1
      C3=(T1*PH20+PO2)*SCAL**3
      C2=-(XN-T2*OH)*SCAL**2
      T3=OH*OH/PO2
      T4=OH*OH/PH20
      T5=OH*OH*OH/(PH20*PO2)
      C1=(T1*XKH2*T3+XKO*T4)*SCAL
      C0=T2*XKH*T5
      C4=0.0
      CALL P4ROOT (C4,C3,C2,C1,C0,R1,R2,R3,R4,IERR)
      X=AIMAG(R1)
      Y=REAL(R1)
      IF (X.EQ.0) GO TO 30
      X=AIMAG(R2)
      Y=REAL(R2)
      IF (X.EQ.0) GO TO 30
      X=AIMAG(R3)
      Y=REAL(R3)
      IF (X.EQ.0) GO TO 30
      WRITE (6,130)
      GO TO 40
```

```
 30 C=Y*SCAL
    H2O=C*PH2O
    O2=C*PO2
    H=XKH*T5/(C*C)
    O=XKO*T4/C
    H2=XKH2*T3/C
    XM=R*(2.*H2O+2.*H2+OH+H)
    WRITE (6,120) NP(I),H2O,O2,H,O,H2,XM
 40 CONTINUE
    GO TO 10
 50 STOP
 90 FORMAT (20I4)
110 FORMAT (6E12.0)
120 FORMAT (I6,1P7E17.6)
```

## II. SUBROUTINE

```
    SUBROUTINE P4ROOT (A,B,C,D,E,R1,R2,R3,R4,IERR)
    COMPLEX R1,R2,R3,R4,ED,EF
    COMPLEX * 16 RE,IM,RI,RJ,P,Q,E1,E2,G1,G2,PARTR,PARTI,
   R,S,T,Q2,Q3
    IERR = 0
    IF (A) 100, 110, 100
110 R4 = 0.
    IF (B) 200,210,200
210 R3 = 0.
    IF (C) 300,310,300
310 R2 = 0.
    IF (D) 381,380,381
380 IERR = 1
    GO TO 500
381 R1 = -E/D
    GO TO 500
300 ASSIGN 360 TO N
    Q2 = D / C
    Q3 = E / C
350 RE =  -Q2/ 2.
    IM =  CDSQRT(RE**2 - Q3)
    RI =  RE + IM
    RJ =  RE - IM
    GO TO N ,(360,410,420)
360 R1 = RI
    R2 = RJ
    GO TO 500
```

```
200 C1 = C/B
    C2 = D/B
    C3 = E/B
    Q = C3/2. - C1 * C2 / 6 . + C1**3 / 27
    P = CDSQRT (Q**2 +(C2 / 3. - C1**2 / 9.)**3)
201 IF (CDABS(P-Q)) 11,10,11
 10 E1 = 0.
    GO TO 12
 11 ED = P-Q
    IF (AIMAG(ED)) 35,30,35
 30 IF (REAL(ED)) 32,10,35
 32 E1 = -1.0 * DEXP(DLOG(CDABS(P-Q)) / 3.)
    GO TO 12
 35 E1 = CDEXP(CDLOG(P-Q) / 3.)
 12 IF (CDABS (-P-Q)) 21,20,21
 20 G1 = 0.
    GO TO 22
 21 EF = -P-Q
    IF (AIMAG(EF)) 45,40,45
 40 IF (REAL(EF))   42,20,45
 42 G1 = -1.0 * DEXP(DLOG(CDABS(-P-Q)) / 3.)
    GO TO 22
 45 G1 = CDEXP(CDLOG(-P-Q) / 3.)
 22 IF (A) 400,26,400
 26 PARTR = -(E1 + G1) / 2. - C1 / 3.
    PARTI = (0,0.5) * DSQRT(0.3D1) * (E1 - G1)
    R1 = E1 + G1 - C1 / 3.
    R2 = PARTR + PARTI
    R3 = PARTR - PARTI
    GO TO 500
100 B = B / A
    C = C / A
    D = D / A
    E = E / A
    E2 = (4. * C * E - (B**2) * E - D**2) / 2. + C *
   (B * D - 4. * E) 1/ 6. - C**3 / 27.
    G2 = CDSQRT (E2 ** 2 + (B * D - 4. * E - C **2 / 3.)
   **3 / 27. )
    P = G2
    Q = E2
    GO TO 201
400 R = E1 + G1 + C / 3.
    S = CDSQRT (B**2 / 4. - C + R)
    T = (B*R - 2.* D) / ( 4. * S**2)
    Q2 = B/2. + S
    Q3 = R/2. + S*T
    ASSIGN 410 TO N
    GO TO 350
```

```
410 R1 = RI
    R2 = RJ
    Q2 = B/2. - S
    Q3 = R/2. - S*T
    ASSIGN 420 TO N
    GO TO 350
420 R3 = RI
    R4 = RJ
500 RETURN
    END
```

UNCLASSIFIED

Security Classification

## DOCUMENT CONTROL DATA - R & D

*(Security classification of title, body of abstract and indexing annotation must be entered when the overall report is classified)*

1. ORIGINATING ACTIVITY *(Corporate author)*
Arnold Engineering Development Center
ARO, Inc., Operating Contractor
Arnold Air Force Station, Tennessee

2a. REPORT SECURITY CLASSIFICATION
UNCLASSIFIED

2b. GROUP
N/A

3. REPORT TITLE

DETERMINATION OF THE EXCITATION REACTION OF THE OH RADICAL IN $H_2$-$O_2$ COMBUSTION

4. DESCRIPTIVE NOTES *(Type of report and inclusive dates)*
Final Report

5. AUTHOR(S) *(First name, middle initial, last name)*
M. G. Davis and W. K. McGregor, Jr., ARO, Inc.
A. A. Mason, The University of Tennessee Space Institute

| 6. REPORT DATE | 7a. TOTAL NO. OF PAGES | 7b. NO. OF REFS |
|---|---|---|
| October 1969 | 86 | 24 |

| 8a. CONTRACT OR GRANT NO. | 9a. ORIGINATOR'S REPORT NUMBER(S) |
|---|---|
| F40600-69-C-0001 | |
| b. PROJECT NO. 4076 | AEDC-TR-69-95 |
| c. Program Element 62403F | 9b. OTHER REPORT NO(S) *(Any other numbers that may be assigned this report)* |
| d. | N/A |

10. DISTRIBUTION STATEMENT
This document has been approved for public release and sale; its distribution is unlimited.

| 11. SUPPLEMENTARY NOTES | 12. SPONSORING MILITARY ACTIVITY |
|---|---|
| Available in DDC | Air Force Avionics Laboratory (AVRO), Wright-Patterson AF Base, Ohio 45433 |

13. ABSTRACT The intensity of the OH radiation from the recombination zone of premixed $H_2$-$O_2$ flames is much greater than can be explained by purely thermal considerations. Previous studies have shown that this extra-thermal radiation can be caused by any one of several chemical reactions. The particular reaction responsible for the overpopulation of the excited levels of the OH radical has been elusive. In this study, by means of analytical examination of previous results together with results obtained in new experiments, all except one of these reactions have been eliminated. The only reaction in the group which successfully fits in the scheme of all observed phenomena is

$$H + OH + OH \rightarrow OH^* + H_2O$$

where OH* refers to the excited A $^2\Sigma^+$. Measurements were made of the OH concentration, temperature, and radiant intensity from the A $^2\Sigma^+ \rightarrow X\ ^2\Pi_1$ (0,0) transition at 3064 Å in several hydrogen lean $H_2$-$O_2$ flames using spectrometric methods. These flames had different equivalence ratios and were diluted with different quantities of diluent gases. Results from these measurements are used together with the chemical reaction rate equation, corresponding to the chemical reaction above, to calculate a value for the OH excitation rate ($K_{IX}$). The value found is $2.3 \times 10^{-32}$ cm$^6$-molecule$^{-3}$-sec$^{-1}$. The errors involved in the measurements and calculations are discussed.

DD FORM 1 NOV 65 1473

UNCLASSIFIED

Security Classification

| 14. KEY WORDS | LINK A | | LINK B | | LINK C | |
|---|---|---|---|---|---|---|
| | ROLE | WT | ROLE | WT | ROLE | WT |
| combustion | | | | | | |
| hydrogen | | | | | | |
| oxygen | | | | | | |
| excitation | | | | | | |
| intensity | | | | | | |
| thermal radiation | | | | | | |
| flames | | | | | | |
| thermochemistry | | | | | | |
| spectroscopy | | | | | | |
| chemiluminescence | | | | | | |
| ultraviolet radiation | | | | | | |
| rocket exhaust | | | | | | |
| chemical radicals | | | | | | |
| radiation measuring instruments | | | | | | |

AFS
Arnold AFB Tenn